Soil degradation assessment across tropical grassland of Western Kenya

John N. Quinton[1*], Gabriel Yesuf[2], German Baldi[3], Mengyi Gong[4], Kelvin Kinuthia[5], Ellen L. Fry[6], Yuda Odongo[7], Barthelemew Nyakundi[7], Joseph Hitimana[7†], Patricia de Britto Costa[6], Alice A. Onyango[5], Sonja M. Leitner[5], Richard D. Bardgett[1,6], Mariana C. Rufino[8†]

[1]Lancaster Environment Centre, Lancaster University, Lancaster, UK.
[2] Rural Payments Agency, Geospatial Services, Reading, UK
[3]Instituto de Matemática Aplicada San Luis –Universidad Nacional de San Luis & CONICET, San Luis, Argentina
[4]School of Mathematical Sciences, Lancaster University, Lancaster, UK
[5]Mazingira Centre for Environmental Research and Education, International Livestock Research Institute, Naivasha Rd, PO 30709, Nairobi, Kenya
[6]Department of Earth and Environmental Sciences, The University of Manchester, Oxford Road, Manchester, M13 9PT, UK.
[7]School of Agricultural Sciences and Natural Resources, University of Kabianga, P.O Box 2030 -20200. Kericho, Kenya
[8]Chair of Livestock Systems, TUM School of Life Sciences, Building 4308, Liesel-Beckmann Straße 4, Freising 85354, Germany

[†]deceased
Correspondence to: John N. Quinton (J.Quinton@lancaster.ac.uk)

Abstract

Soils across sub-Saharan Africa are exposed to extensive degradation processes, which can reduce~~cing~~ their ability to produce crops and support livestock. While there has been a significant research effort focussing on soil degradation in sub-Saharan croplands, less research effort had been directed towards grasslands. Here, we tested the effectiveness of remote sensing to classify the soil degradation status of smallholder grazing lands. Focussing on grasslands used by smallholders in the districts of Nyando and Kuresoi in Western Kenya, we first used remote sensing (RS) to classify grasslands as productive grazing lands, grazing lands that followed a variable trend in vegetation productivity (transition), and unstable and unproductive (degraded) ~~and~~ grazing lands. We then ~~that followed a variable trend in vegetation productivity (transition)either equilibrium, transition or degraded, and then~~ tested how this classification related to measured soil parameters indicative of soil degradation. We then used this classification, which was based on a temporal analysis of Normalised Difference Vegetation Index (NDVI), Enhanced Vegetation Index (EVI) and Normalised Difference Water Index (NDWI) between 2013 and 2018, to identify 90 field sites across the two districts, which we then sampled and analysed for a range of physical, chemical and biological soil properties. Only soil microbial biomass carbon (C) showed consistent alignment with the RS classification, although there was some overlap with other soil parameters at one or other of the ~~sites~~study areas. To group the sites using the soil ~~parameters~~variables, which we split by ~~district~~ study area and into stable (those that are slow to change) and transient (those that change rapidly i~~n~~n response to a changing

pedological environment) ~~soil variables~~, K-means clustering was undertaken. Two clusters were produced for each district. One of these clusters ~~d. One of the clusters~~ included sites with higher levels of C, nitrogen (N), phosphorus (P) and pH, that aligned well with the RS classification at Kuresoi, with seven out of ten ~~equilibrium~~ productive sites being assigned to this cluster. The ~~. The~~ other cluster included sites ~~cluster, in~~ with ~~Nyando, had~~ high soil C and N~~P~~, but low pH and relatively low soil bulk density, and corresponded to 12 out of the 16 ~~equilibrium~~ productive sites in Nyando. Overall, our results suggest that while the use of RS methods for classifying degraded grasslands and the soils supporting them does have significant advantages in terms of time and costs over field survey, supplementing these methods with a limited set of soil parameters related to nutrient cycling, such as microbial biomass C, soil P, percent C and N, and soil pH, could enhance our ability to identify degraded soils and target restoration efforts.

Introduction

Approximately 660 million hectares of sub-Saharan African (SSA) soils are estimated to be degraded, which represents a significant portion of the global extent of degraded soils (Gibbs and Salmon, 2015). Soil degradation reduces the functioning of soils and is a result of multiple processes including soil erosion by wind, water and tillage, salinisation, nutrient depletion, and compaction (Bridges and Oldeman, 1999) and may be triggered by shifts in land use, management or climatic changes. Most attention has been placed on the impacts of soil degradation on food security, and it has been cited as the leading cause of stagnation in food production, creating uncertainties for income and nutritional security for rural populations (Barbier and Hochard, 2016). Reduced plant productivity associated with degraded soil also reduces the input of carbon (C) to the soil leading to lower C stocks (Bai and Cotrufo, 2022) and less biomass to support livestock. Further, when grazing lands are degraded, farmers are often forced to graze their livestock in adjacent forests, which can negatively affect forest plant communities (Mullah et al., 2023). Thus, restoring degraded soils has become a priority for securing future food supply while simultaneously avoiding biodiversity and C losses. This has resulted in several initiatives supporting landscape restoration in Africa, notably the African forest restoration initiative (Messinger and Winterbottom, 2016), which gathered commitments from African governments to restore 100 million hectares of degraded land by 2030.

The East African highlands of Kenya are densely populated areas of high agro-ecological potential. Farms here are small, typically smaller than 2 hectares (Lowder et al., 2016). Production includes a mix of grains and vegetables for local consumption, some cash crops, such as tea (*Camellia sinensis* (L.) O. Kuntze), and livestock keeping. Milk from livestock is important to smallholder families as a valuable source of protein in a protein-poor diet (Hulett et al., 2014). Grazing animals are also culturally significant, reflecting the social standing of the owner and providing meat for celebrations and an additional source of cash when sold (Moll, 2005). Smallholder systems in the highlands of Kenya have a range of stocking rates, typically expressed in Tropical Livestock Units (TLU) per hectare. ~~, for example~~ Stocking rates in ~~in~~ the Kenyan highlands are reported to be between 1 and 1.4 TLU ha^{-1} ~~are reported~~ depending on the nature of the system (Bebe et al 2003), whereas for Murang'a County to the south east of our study area, they are ~~-~~3-6 TLU ha^{-1} (Ortiz-Gonzalo et al, 2017) and for dairy cattle in Kiambu County to the west of our study area an average of 2.1 TLU ha-1 (Were et al 2025). ~~Grazing~~

~~animals include sheep, goats and cattle, and animal numbers range between 5-10 sheep and goats, and 1-2 cattle per hectare.~~ Additionally, grazing takes place on farms and on utility areas, which are controlled by local institutions; these often come under higher greater pressure because multiple livestock owners have access to the land. In response to these pressures, grassland soil degradation is widespread in Kenya (Nzau et al., 2018) although we know little about its extent and severity.

Given the importance of grazing land for sustaining rural livelihoods it is surprising that globally, and particularly in SSA, much less recent research attention has been placed on understanding degradation of grazing lands (Bardgett et al., 2021), ~~particularly in SSA~~. High grazing pressures can degrade soil fertility with associated declines in soil properties underpinning soil health (Pelster et al., 2017), for instance causing soil compaction and reducing soil infiltration rates (Owuor et al., 2018) and C inputs to soil due to the removal of plant material by livestock and reductions in root mass (Zhou et al., 2017). Further, catchments with high livestock densities have larger nutrient and sediment loads in streams (Jacobs et al., 2017), have greater emissions of greenhouse gases (Arias-Navarro et al., 2017), and increase the risk of forest degradation (Brandt et al., 2018). Low soil nutrient availability and the deterioration in soil physical properties impairs plant growth and alters plant nutrient concentrations (Augustine et al., 2003), and reduces organic matter return to soil. With poorer vegetation cover and lower organic matter contents, soils become increasingly vulnerable to erosion, leading to lower ~~less~~ soil depth and organic matter, which further reduces water and nutrient retention (Quinton and Fiener., 2024). This leads to a downward spiral of productivity loss and reduced capacity of systems to resist and recover from climate extremes (Quinton and Fiener., 2024; Van De Koppel et al., 1997).

The UN Decade (2021-30) on ecosystem restoration (Unep, 2019) has focused attention on understanding where and how severely soils are degraded and whether they can recover, which is clearly important for the design of restoration programmes. In grazed systems, soil degradation is often recognised by the presence of bare soil. However, using bare soil as an indicator can be problematic in systems where erratic rainfall patterns lead to seasonal and inter-annual fluctuations in vegetation growth coupled with reduced vegetation cover due to grazing (Ellis and Swift, 1988). In such environments, poor vegetation growth may or may not indicate degraded soils. However, utilising the response of vegetation to changed soil properties and water availability is an approach that has been used by several authors (e.g. Eckert et al., 2015; Zhou et al., 2017).

Here, we tested the reliability of remote sensing approaches for classifying degradation status of smallholder grazing land and compared it with an approach based on the sampling of soils and characterisation of soil properties related to soil structural stability and C, nitrogen (N) and phosphorus (P) cycling. Working in two areas representing smallholder grazing land of western Kenya (Nyando and Kuresoi), we assessed degradation using a dynamic multi-year approach to derive a range of metrics to quantify the magnitude, seasonality and interannual variability of the vegetation (Rufino et al., 2016), and then tested whether or not the classification was related to measured soil parameters. We then explored whether soil variables classified as either stable or transient could be used to classify soil degradation status in grasslands.

Methodology

Field areas

We used a comparative landscape-level analysis of two agro-ecosystems with different ecologies (Figure 1). The ~~sites~~ study areas are in western Kenya covering the neighbouring basins of the rivers Sondu-Miriu and Nyando spanning land use transitions from East African montane forests to grasslands and croplands. Study area ~~Site~~ 1 (Kuresoi) is in Kericho county located in the Sondu river basin in the proximity of the Mau Forest, at an altitude ranging from 1,~~700~~ 688 to ~~3,000~~2947 masl, a mean slope of 7.6 degrees, with an average rainfall of 1,988±328 mm. The geology originates from the early Miocene, with phonolites dominating in the lower part of the catchment, and phonolitic nephelinites in the upper part. The topography is rolling with moderate slopes-. -A variety of Tertiary tuffs are found on the highest part of the Mau Escarpment (Jennings, 1971). Study area~~Site~~ 2 is in Lower Nyando located in the Nyando river basin, with an average rainfall of 1,150 mm and spanning from the foot of a plateau at 1,~~600~~ 781 towards Lake Victoria at 1,~~200~~ 170 masl, with a mean slope of 5.3 degrees. Topography is gently sloping towards ephemeral and permanent drainage. Soils are derived from Holocene alluvial deposits, and a variety of parent materials including phonolites and granitic gneisses (Iuss, 2015). The Lower Nyando study ~~site~~ area covers an area which is approximately 160 km^2, whilst the Kuresoi ~~site~~ study area covers an area that is approximately 1,300 km^2 next to the Mau Forest. More details on land use and vegetation are given below.

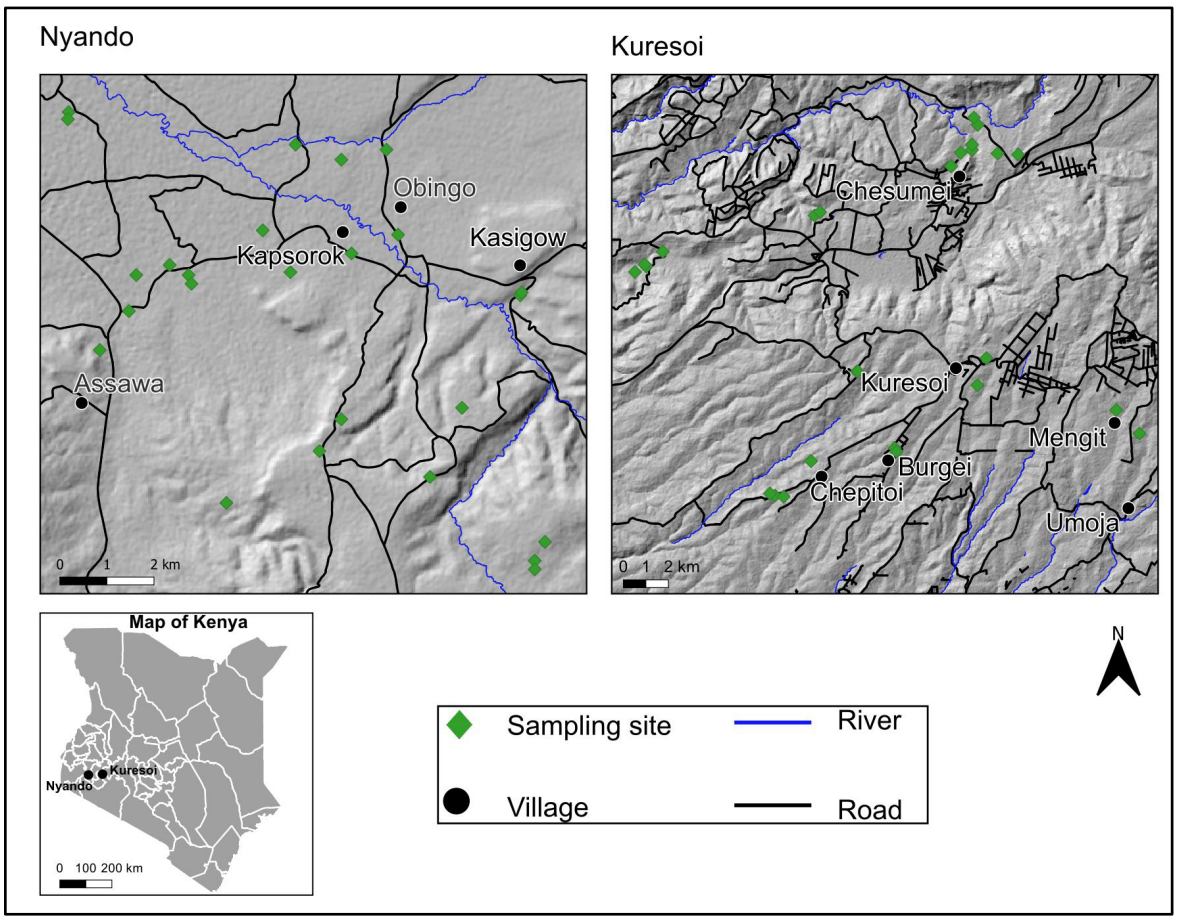

Figure 1: Location ~~map showing~~of ~~project sites~~study areas in Kenya (bottom left) and expanded views of Kuresoi (top right) and Lower Nyando (top left). Map produced using

~~Arc~~QGIS® software ~~by Esri~~. Road network, river and settlement were reproduced using OpenStreetMap vector data. Accessed on 2019-06-09 and are licensed under the Open Database 1.0 License. Digital Elevation Model was produced using ASTER Global Digital Elevation Model (GDEM) 30-meter resolution as input and under license from NASA Earth Science Information Partners Data Preservation and Stewardship Committee. 2019. Earth Science Data. Ver. 2.

Approach to degradation classification

~~The first step to define~~Our approach to classifying grasslands focusses on the rate at which greening takes place following a dry season (Yu et al., 2012) . We define ~~degradation states followeding the concepts developed by (Briske et al., 2003)~~productive grasslands are those where biomass productivity is higher and returns rapidly following dry seasons. On the other hand, degraded grasslands are those with lower peak biomass and which display ~~only~~ slow~~ly~~ recovery following drought. Those grasslands that are intermediatory, displaying ~~which exhibit~~ characteristics of both productive and degraded grasslands, are~~nd~~ termed transition. These states are defined using an ~~involved an~~ analytical approach using remote sensing images of both study ~~sites~~areas which is set out in the following sections.~~.~~ This spatio-temporal analysis covered a period of 5 years (2013 – 2018)~~, where productive grazing lands were classified as being in equilibrium, grazing lands that followed a variable trend were defined as transition, and degraded grazing land were those shown as unstable and unproductive~~.

Remote sensing data selection

To analyse the structural characteristics of grasslands supporting smallholder communities in Kuresoi and Lower Nyando, we implemented time-series seasonal analysis that ~~and~~ classified~~y~~ landscape-level stages of degradation. We used~~,~~ 35 satellite image scenes ~~were collected~~ from the archives of European Space Agency (ESA 2016) and United States Geological Surveys (https://earthexplorer.usgs.gov/) (Table 1). The selection of different sensors was necessary to: i) fill missing dates from the Sentinel collection which had the higher~~st~~ spatial resolution, but shorter temporal resolution and ii) to maintain~~attain~~ consistency in annual seasonal sampling between 2013 and 2018. The final satellite imagery was from Landsat-Thematic Mapper (TM) L2, Landsat Operational Land Imager (OLI) L2 and Sentinel-2 sensors L2A. Level 2 images are Analysis Ready Data (ARD) ~~-~~and ~~are~~atmospherically corrected surface reflectance and ~~temperature~~ data and therefore free from ~~without~~ the effects of haze and water vapour. Landsat-TM and OLI imagery have a spatial resolution of 30 m, while Sentinel-2 imagery has a spatial resolution of 10 m.

The decision to select and process high-resolution imagery is due to the focus on smallholder dairy farms, which are associated with grazing lands that are often less than 1 ha and therefore easier to detect with higher resolution imagery. For LandSat-TM scenes, we downloaded blue (band 1), red (band 3), near-infrared (band 4), and shortwave infrared (band 6) spectral bands from USGS earth explorer repository. For Landsat-OLI scenes, we downloaded blue (band 2), red (band 4), near-infrared (band 5) and shortwave infrared (band 6). For the Sentinel-2 scenes, we downloaded blue (band 2), red (band 4), near infrared (band 8) and shortwave infrared (band 11). We loaded the individual bands into RStudio using the raster package. All Landsat images were resampled to 10 m using Sentinel-2 images as reference. This is because TIMESAT 3.3

(see description of use below), which is a program for analysing time-series of satellite derived index data by extracting seasonal parameters (Eklundh and Jönsson, 2015) and ~~(see below)~~ requires all input image scenes to have the same spatial resolution when creating raster stacks and before model fitting ~~to the data~~. ~~No further image enhancements were applied because TIMESAT algorithm accounts for missing data and quality flags resulting from cloud and aerosols~~ No further image enhancements were applied because TIMESAT algorithm reduces negative biases arising from cloudiness by fitting the model to the upper envelope of the vegetation/water index data (Eklundh and Jönsson, 2015). Despite these corrections, TIMESAT is unable to reduce negatively biased residuals related to surface anisotropy and sensor defects. However, we did not detect the effects of sensor defects in this analysis. ~~Afterwards, we divided the difference and sum of near-infra red and red bands to derive estimates of NDVI values per pixel (Equation 1), and divided the difference and the sum of near-infrared and shortwave infrared to derive estimates of NDWI per pixel (Equation 3). Furthermore, we applied correction factors as we divided the difference between near-infrared and red bands from near-infrared to derive estimates of EVI for each pixel (Equation 2~~ Afterwards, we calculated NDVI values in each pixel by dividing the difference with the sum of near-infra red and red bands (Equation 1).To derive EVI values in each pixel, we applied correction factors and divided the difference between near-infrared and red bands with near-infrared band (Equation 2). We calculated NDWI in each pixel by dividing the difference with the sum of near-infrared and shortwave infrared (Equation 3).

Table 1: Summary of dates of acquisition of Landsat and Sentinel-2 imagery used for the determination of Normalized Difference Vegetation Index, Enhanced Vegetation Index and Normalized Difference Water Index.

2013	2014	2015	2016	2017	2018
NA	2014/01/25[1]	2015/01/12[1]	2016/01/08[2]	2017/01/12[2]	2018/01/22[2]
2013/04/28[1]	2014/04/01[1]	2015/04/02[1]	2016/04/27[2]	2017/04/02[2]	2018/04/10[1]
2013/06/17[1]	2014/06/18[1]	2015/06/07[1]	2016/06/06[2]	2017/06/11[2]	2018/06/11[2]
2013/08/18[1]	2014/08/21[1]	2015/08/11[2]	2016/08/25[2]	2017/08/20[2]	2018/08/05[2]
2013/10/05[1]	2014/10/25[1]	2015/10/25[1]	2016/10/29[1]	2017/10/29[1]	2018/10/03[1]
2013/12/24[1]	2014/12/11[1]	2015/12/29[2]	2016/12/23[2]	2017/12/28[2]	2018/12/18[2]

[1] Landsat Thematic Mapper (TM) or Operational Land Imager (OLI) imagery
[2] Sentinel-2 imagery

Note: Landsat images were resampled to 10m resolution.

~~To classify degradation status, 35 satellite image scenes were collected from the archives of European Space Agency (Esa, 2016) and the United States Geological Surveys earth explorer (Usgs, 2025) (Supplementary Table S1). The selection of different sensors was necessary to fill missing dates from the Sentinel collection which had a higher spatial resolution (10 m) but has been deployed in space for a shorter period (since 2015) compared to the Landsat sensors. The final satellite imagery was from Landsat-Thematic Mapper (TM), Landsat Operational Land Imager (OLI) and Sentinel-2~~

~~sensors. Landsat-TM and OLI imagery have a spatial resolution of 30 m. The mapping of grasslands in smallholder production systems required high-resolution imagery because of the relatively small sizes of the fields, which are often less than 1 ha. Therefore, the Landsat-derived images were resampled to 10 m using the Sentinel-2 imagery as reference.~~

Temporal and seasonal analysis

Three vegetation indices, Normalised Difference Vegetation Index (NDVI), Enhanced Vegetation Index (EVI) and Normalised Difference Water Index (NDWI) were calculated using blue, red, near infra-red (NIR), and shortwave infra-red bands (Equations, 1, 2 and 3). These indices were selected because vegetation and water indices are effective to estimate changes in ecosystems (He et al., 2018) and grassland biomass (Todd et al., 1998), distinguish canopy density (Huete et al., 1997), and characterise drought (Rulinda et al., 2012).

$$NDVI = \frac{(NIR - Red)}{(NIR + Red)} \quad (1)$$

$$EVI = G * \left[\frac{(NIR - Red)}{(NIR + C1 * Red - C2 * Blue + L)}\right] \quad (2)$$

$$NDWI = \frac{(NIR - SWIR)}{(NIR + SWIR)} \quad (3)$$

where *NIR* is near-infra red; *G* represents a gain factor; *L* adjusts for canopy background; C_1 and C_2 are coefficients for atmospheric resistance (G = 2.5, C_1 = 6, and C_2 = 7.5). Applying these coefficients allows for index calculation as a ratio between Red and *NIR* values, while reducing the background noise, atmospheric noise, and data saturation. Index values were calculated on a scale of -1 to 1.

The seasonality of the vegetation was interpolated using TIMESAT v3.3 algorithm (Eklundh and Jönsson, 2015). An adaptive Savitzky-Golay smoothed function was fitted over the index time-series data of Lower Nyando to model bi-modal seasons and to determine the timings of the growing seasons. A double gaussian function was fitted over the index time-series data of Kuresoi to model seasonal peaks where the vegetation dynamics is less variable. The adaptive function of TIMESAT modelled abrupt changes in vegetation effectively, which was often the case in the Lower Nyando landscape consisting of an intricate mosaic of land covers. A double logistic function allowed to isolate noise (e.g. caused by clouds) in Kuresoi data. To capture seasonal peaks, the functions were fitted to the upper envelope of the time-series following Eklundh and Jönsson (2015). After fitting the statistical functions to the data, the following seasonal parameters were estimated: Seasonal Amplitude (Amp), Start of Season (StoSt), End of Season (EoS), Function value at Start of Season (SoSv), Function value at End of Season (EoSv), Season Length (Len), Base level, Mid of the Season (Mid), Largest data, Maximum Value (MV), Left Derivative/greening rates (LD/GR, and Right Derivative/browning rates (RD/BR), Large Seasonal Integral and Small Seasonal Integral. For definitions of seasonal parameters and further explanations see (Eklundh and Jönsson, 2017).

Degradation units' classification

Six seasonal parameters were selected for the classification of degradation units: SoSv, EoSv, MV, GR and BR because of the phenology characteristic of the ecosystems under study (Kong et al., 2022). Productive v~~V~~egetation ~~at equilibrium~~ state was expected to have higher values for SoSv, EoSv, MV and experience faster greening compared to

vegetation of the units with transition and ~~regime-shift~~degraded states (Xiao et al., 2006; Yu et al., 2012). There are no predefined seasonal parameter values that define ~~the~~ stages of grassland degradation in Western Kenya, as there are for ~~in~~ other African grasslands (~~-~~e.g. ~~. For instance,~~ Tagesson et al. (2015) quantified maximum NDVI values between 0.59 and 0.82 for different grasslands in a semi-arid region of Senegal). Therefore, thresholds were ~~defined~~generated for five potential models using the average distribution of the selected seasonal parameters (Table 2~~1~~). Thresholding was implemented using written functions in R to partition parameter values into three groups corresponding to ~~equilibrium~~productive, transition, and ~~regime-shifts~~degraded. However, ~~Several models were generated using different combinations of seasonal parameter classifications (Table 1). However, o~~only ~~two models~~Model 3 and 5 were visually consistent with the spatial distribution of dominant land cover types (e.g., large forest patch). All land cover types were retained during seasonal parameter estimation and classification to allow for accurate seasonal models of the ~~sites~~study areas. Using the above approach and thresholds, productive vegetation ~~at equilibrium state~~ was assigned to high MV(>0.8), high GR (>0.5), and low BR (<0.3). Vegetation at the ~~regime-shift state~~degraded state had low MV (<0.5), low GR (≤0.8), and high BR (~~≤~~≥ 0.5) and transition grasslands were those falling between these values. Finally, the classification from each index was combined to determine areas of common agreement and produce maps identifying productive, transition, and degraded areas (Figure 2).~~.~~

Table 2~~1~~: Summary of models' description, seasonal parameters and threshold values used for degradation unit classification of Lower Nyando and Kuresoi. Model 3 and 5 were the best performing models based on a visual assessment.

Description	Index	Threshold values (Nyando)§					Threshold values (Kuresoi)§				
		MV	SoSv	EoSv	GR	BR	MV	SoSv	EoSv	GR	BR
Model 1	NDVI	0.54	0.55	0.55	0.58	0.56	0.81	0.78	0.81	0.8	0.78
	EVI	0.49	0.5	0.49	0.54	0.54	0.75	0.76	0.76	0.79	0.74
	NDWI	0.81	0.79	0.79	0.77	0.81	0.83	0.82	0.82	0.79	0.80
Model 2	NDVI	0.54	0.55	0.55	0.58		0.81	0.78	0.81	0.80	
	EVI	0.49	0.50	0.49	0.54		0.75	0.76	0.76	0.79	
Model 3*	NDVI	0.54	0.55	0.55			0.81	0.78	0.81		
	NDWI	0.81	0.79	0.79			0.83	0.82	0.82		
Model 4	EVI	0.49	0.50	0.49	0.54	0.54	0.75	0.76	0.76	0.79	0.74
	NDWI	0.81	0.79	0.79	0.77	0.81	0.83	0.82	0.82	0.79	0.80
Model 5**	NDWI	0.81	0.79	0.79			0.83	0.82	0.82		

~~* More consistent classification of degraded grasslands and bare grounds as regime-shift in Nyando~~

~~** More consistent classification of grasslands at equilibrium in Kuresoi~~

~~§ Threshold values represent the average distributions.~~

Selecting sampling locations

~~Through visual inspection, model 3 and model 5 were found to be the most consistent with Google Earth Images of the sites. Subsequently, the~~ L~~l~~and cover data from the European Space Agency Climate Change Initiative land cover vector layer (ESA 2016) was used to mask forests, urban and water bodies to detect grazing areas. Afterwards, locations were selected using the Fishnet tool of ArcGIS. Stratified random sampling was used to create sampling locations separated by a minimum distance of 1 km to select approximately 30 sampling locations for each degradation unit, resulting in 100 sampling locations including replacements. ~~The status~~Locations land that coincided with recently cultivated areas (<10 years) and/or road tracks ~~of the locations was checked visually in~~ were removed following examination using Google Earth (2008 - 2018) ~~to remove locations that coincided with recently cultivated areas (<10 years) and/or road tracks~~. Locations that had signs of recent cultivation or tillage lines were excluded. In October-November 2019, the locations were visited to remove sample locations that were inaccessible or when landowners denied access. In total, 90 sites were ~~finally~~ selected for study ~~after land use history checks and obtaining consent of farmers/landowners~~ (Figure 2).

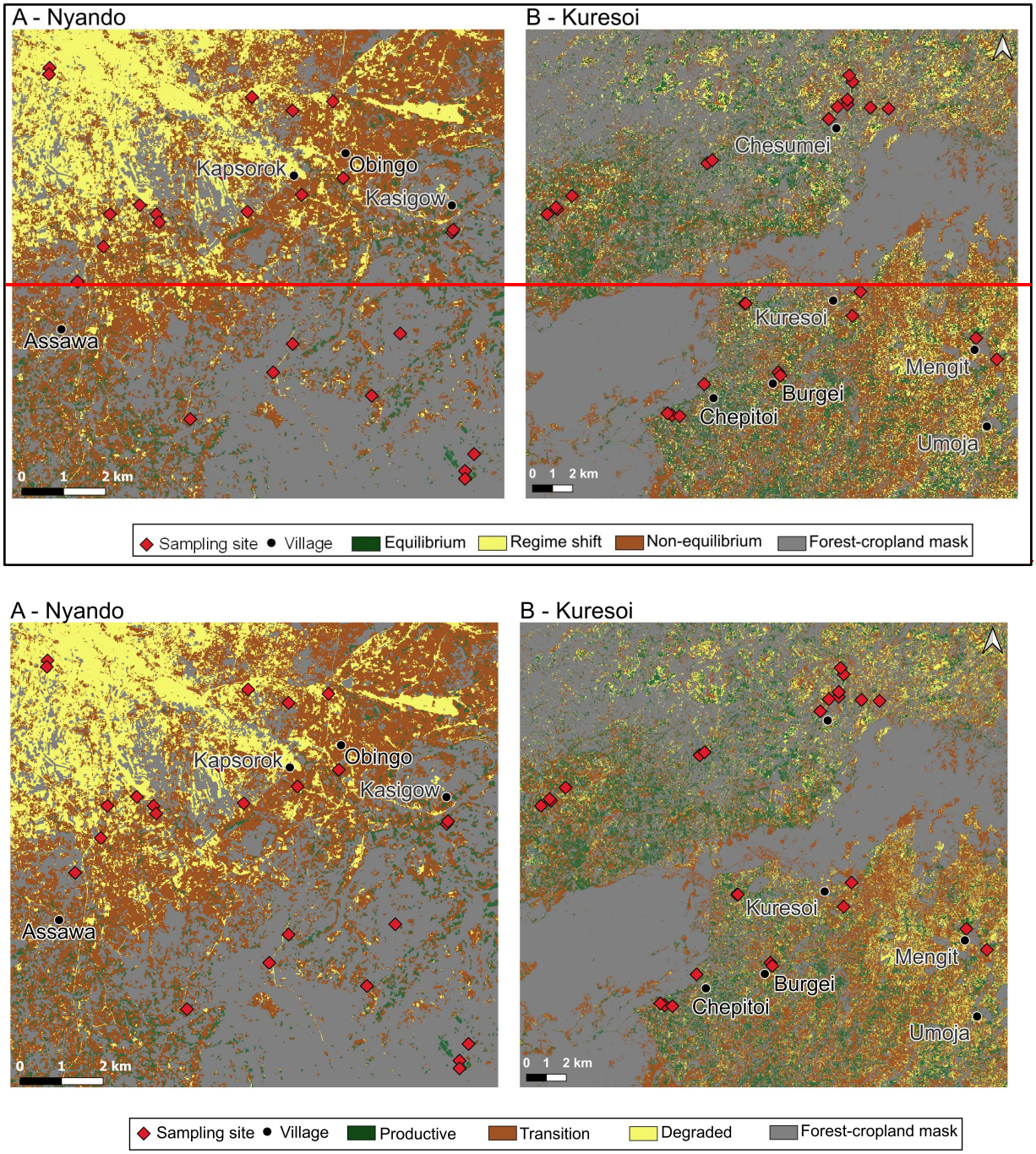

Figure 2: Classification of Lower Nyando (A) and Kuresoi (B) ~~project sites~~study areas into three ERUs: ~~equilibrium~~productive, transition and regime-shift. Sampling sites are overlaid and show the distribution of field experiments and locations of soil and aboveground biomass samples. Map produced using ~~Arc~~QGIS® software ~~by Esri~~. ~~Road s~~Settlement information were reproduced using OpenStreetMap vector data. Accessed on 2019-06-09 and are licensed under the Open Database 1.0 License. .

Soil sampling and analyses

Soils at each site were sampled to 10 cm depth and analysed for a range of physical, chemical and biological parameters (Table 3~~S1~~).

Bulk density was calculated following sampling of intact soil with 45 mm diameter rings and soil texture was determined by laser diffraction (Beckman-Coulter LSI3 320), after soil dispersion in sodium hexametaphosphate. Aggregate stability was determined using the fast-wetting method of aggregate stability (Le Bissonnais, 1996), which subjects the

aggregates to rapid immersion in water for 10 min. After that, aggregate samples were sieved in ethanol before oven drying to determine final aggregate size distribution, producing a mean weight diameter (MWD).

For each site sampled ~~plot~~ we measured total soil C, N, P, and selected microbial-mediated functions related to nutrient cycling . These were microbial biomass (C and N), nutrient availability (i.e. soluble inorganic and organic N and P pools, and dissolved organic C), rates of N mineralisation and nitrification. ~~, and a suite of extracellular enzyme activities involved in the degradation of cellulose, chitin, lignin and proteins (i.e. β-glucosidase (GLC), cellobiohydrolase (CBH), β-xylosidase (XYL), N-acetylglucosaminidase (NAG), phosphatase (PHO), phenol oxidase (POX), peroxidase (PER), and urease (URE)), following Fry et al. (2018) and De Vries and Bardgett (2016), and as described in Broadbent et al. (2022) for extracellular enzymes.~~

Briefly, percentage C and N in dry, ground soil were measured using an elemental combustion analyser (Elementar Vario EL, Hanau, Germany). We measured dissolved total and organic C (DC and DOC respectively), plant available nitrate (NO_3^-) and total dissolved N (TDN) by weighing 5 g of fresh soil accurately and shaking in 35 ml Milli-Q water for 10 minutes at 150 rpm, before filtering through Whatman 42 filter paper. C in the filtrate was quantified using an Aurora 1030W TOC analyser (OI Analytical, UK), and N was quantified using an autoanalyser (AA3, Seal Analytical, Wrexham UK). Organic N was calculated by subtracting inorganic N values (nitrate and ammonium) from total N. pH of the filtrate was determined using a pH probe (Mettler Toledo FE20, Salford, UK). Values were adjusted for soil moisture. Soil ammonium (NH_4^+) was measured by shaking 5 g of fresh soil in 25ml 1M KCl for 30 minutes, extracting through Whatman 1 filter paper and analysing on the autoanalyser as before. For potential mineralisation and nitrification, 5 g of each soil sample was incubated for 14 days at 25 °C before being extracted and analysed for NH_4^+ and NO_3^- using the KCl procedure. The values from the initial KCl extraction (summed NH_4^+ and NO_3^-) were subtracted from the day 14 extraction and divided by 14 to give a rate of potential mineralisation per day. Nitrification was calculated by using the NO_3^- values only. Negative values imply denitrification, i.e. loss of N as N_2 gas. Microbial biomass C and N were determined using the chloroform-fumigation method (Vance 1987). We weighed 5 g of each sample twice. The first replicates were shaken in 25 ml 0.5M K_2SO_4 for 30 minutes, before passing through Whatman 42 filter paper. The second were placed in a desiccator containing a beaker of chloroform under vacuum for 24 hours to lyse microbial cells, before being extracted as before. Total dissolved C and total extractable N were analysed using the Aurora and the autoanalyser respectively. Microbial biomass C and N were calculated by subtracting the unfumigated values from the fumigated ones.

Total soil P was measured using the Kjeldahl digestion method (Kjeldahl, 1883). We mixed 420 ml concentrated sulfuric acid with 12 g lithium sulphate. We added 0.5 ml of this mixture to 50 mg of dry ground soil per sample in glass digestion tubes. We then added 0.5 ml 30% hydrogen peroxide. Samples were heated at 200°C, then we added a 50°C heat increase every 30 minutes until it reached 360°C. Samples were heated at 360°C for two hours before cooling. When cool, 0.5ml of hydrogen peroxide was added and samples were digested at 360°C for a further two hours. Samples were diluted to 50 ml using Milli-Q water. They were analysed using the ascorbic acid microplate method after (Kuo, 1996), where samples were measured colourimetrically at 880 nm. For inorganic P, we placed 2g of dry soil into a falcon tube with 50ml of 0.5M sulfuric acid. This was shaken at 150rpm for 16 hours. The samples were centrifuged at 1500 rpm for

10 minutes, and the supernatant was analysed using the ascorbic acid method (Olsen and Sommers, 1982).
In addition, a suite of extracellular enzyme activities involved in the degradation of cellulose, chitin, lignin and proteins (i.e. β-glucosidase (GLC), cellobiohydrolase (CBH), β-xylosidase (XYL), N-acetylglucosaminidase (NAG), phosphatase (PHO), phenol oxidase (POX), peroxidase (PER), and urease (URE)), were determined which added artificial p-nitrophenyl (pNP) linked substrates to induce a colour reaction through p-nitrophenyl production following Fry et al. (2018) and De Vries and Bardgett and as described in Broadbent et al. (2022).

Description of the data set

For testing and clustering analysis, we focused on a total of 28 soil variables measured from the soil samples collected from the 0-0.1m depth in Kuresoi and Nyando. ~~, respectively.~~ These variables were grouped in relation their rate of change in response to degradation as either ~~stable~~ stable (changes over multi-year time periods) or transient (changes over seasonal time periods~~-~~) soil variables ~~and relate to the rate of change of these parameters in response to degradatio~~Bulk~~n. Changes in bulk~~ density and soil hydraulic properties ~~can persist~~change over ~~seasonal to~~ multi-annual, ~~-~~timescales (Berisso et al., 2012), as can contents of C (Tully et al., 2015), N (Sun and Chen, 2025) and P along with pH (Tully et al., 2015), and thus were considered stable. Other soil physical variables (percentage ~~aggregate stability,~~ sand ~~percentage~~, silt ~~percentage~~, and clay, ~~percentage;~~ and aggregate stability) were also considered stable. We reason that that as aggregate stability is strongly related to soil texture and organic matter (Kemper and Koch, 1966) both variables that change slowly, that aggregate stability will also change slowly, although there is little literature evidence to support this. ~~(Kemper and Koch, 1966)hence, these parameters were considered to be stable soil variables.~~ In contrast, soil biological parameters, including enzyme activities, microbial biomass, and rates of nutrient mineralisation, respond rapidly to change in response to seasonal changes environmental conditions (Cordero et al., 2023) and therefore soil enzymes (PHO, GLC, NAG, XYL, CBH, PER, POX, URE), water extractable NO_3, and KCl-extracted NH_4, microbial C, microbial N, total dissolved C, organic dissolved C, mineralisation and nitrification were considered transient.
~~Finally,~~ The statistical analysis for investigating the difference between degradation classes were carried out on the 28 variables across all 45 sites in Kuresoi and Nyando respectively. For the clustering analysis, the sites with incomplete data (i.e., with missing observation in any of the variables in the stable or transient variable sets) were removed, resulting in 31 sites in Nyando, 41 sites in Kuresoi for the stable variables, and 42 sites in Nyando, 38 sites in Kuresoi for the transient variables. The ~~distribution~~ number of sites in each degradation ~~states~~ class ~~of these sites is summarised~~is given in Table 3~~S2~~.

Statistical analysis of field data

Statistical analyses were carried out to investigate differences in field sampling data between sites with different degradation labels allocated from remote sensing (Table 2). The analyses were applied to the data from Kuresoi and Nyando respectively. First, analysis of variance (ANOVA), with the soil variables being the response and the degradation class labels being the explanatory variable, was applied to ~~all~~ soil variables which follow approximately a normal distribution, according to Shapiro-Wilks test. This is to identify any mean differences between the degradation classes ~~within Kuresoi and~~

~~Nyando respectively~~. For variables that failed the normality test (i.e., having more than one degradation classes that are not normally distributed), the non-parametric Kruskal-Wallis test was used. For soil variables with a significant mean difference, ~~t-test~~ further pairwise comparison tests were~~as then~~ applied to each pair of degradation classes (i.e.~~e.g.~~, ~~equilibrium~~ productive ~~vs.~~vs. degraded, productive vs transition, transition vs.~~.~~ degraded)~~ to further investigate the content of the mean differences~~. ~~In particular,~~ ~~Tukey's~~Tukey's honest significant difference (HSD) test was used for parametric testing and Wilcoxon rank test was used for non-parametric testing.~~ The results are presented as the letter-based display in brackets in Table 2. Boxplots of the variables with significant difference between degradation classes at p<0.1 level are shown in Figure 3.~~

Description of the clustering methods

Considering the features of our data sets, i.e., relatively large number of variables (12 and 16 for stable and transient variables respectively) as compared to the number of sites (between 31 to 42) in each area~~ and~~, relatively high variability in some variables, and ~~the~~ initial experiments with different clustering methods, we chose to use k-means clustering for our main analysis. In particular, the k-means clustering was applied to the principal components extracted from the data. ~~We also applied the Gaussian mixture model to the data sets, but only for reference.~~ Below we briefly introduce the clustering method~~s~~ and provide some details on the approach we took.

K-means clustering is a popular method for grouping a population of n subjects (n being the number of sites in this case), each of p-dimensional (p being the number of covariates), into a number of k clusters, using algorithms developed by e.g. ~~,~~Hartigan and Wong (1979); Lloyd (1957); Macqueen (1967)~~. and. Gaussian mixture model is another popular clustering approach. It is a model-based clustering method introduced by~~ Fraley and Raftery (2002)~~., where it assumes that the population follows a mixture of k p-dimensional Gaussian distributions.~~ Few assumptions are required for applying the k-means algorithm, although it has been acknowledged that the method works better with clusters that are of similar shapes or sizes (Steinley, 2006). The result can be sensitive to outliers (Johnson and Wichern, 2007). ~~In contrast, a Gaussian mixture model needs specific assumptions on the covariance structure, some of which involve the estimation of a large number of parameters and hence is not suitable for a small sample size. Considering these features, k-means clustering seems to be a more suitable choice over Gaussian mixture model when it comes to data sets with high dimensionality, high variability and relatively small sample size.~~

To determine the number of clusters for k-means clustering, methods such as elbow plot of the total sum of squared distance between points and cluster centres and gap statistics (Tibshirani et al., 2001) can be used. ~~For Gaussian mixture model, Bayesian information criterion (BIC) can be used to select cluster numbers~~ (Scrucca et al., 2023)~~, providing a more objective solution. Due to the relatively small population size in this analysis, only cluster numbers from two to five were investigated. Based on the model selection criteria, after taking the robustness of the clustering results into account and discounting the cluster numbers thatced singletons (i.e., one site as a group of its own), the cluster number was settled to be two for both stable and transient variable sets in Kuresoi and Nyando, respectively.~~

~~Due to the relatively large number of variables (p) as compared to the relatively small number of sites (n)~~, To begin with, principal component analysis (PCA) was ~~first~~ applied to reduce the dimension of the data. The number of principal components (PCs) was

selected to account for at least 80% of the variation~~information~~ in the data~~, or the correlation matrix to be precise~~. This resulted in ~~a much smaller number (six) of "variables" in the form of PCs~~ six PCs each for the clustering of stable and transient variables from Kuresoi and Nyando respectively~~to be used in the clustering analysis~~, which helped to improve the stability of the clustering algorithms. ~~-~~Due to the relatively small population size in this analysis, only cluster numbers from two to five were investigated. Based on the model selection criteria, after taking the robustness of the clustering results into account and discounting the cluster numbers that resulted in singletons (i.e., one site as a group of its own), the cluster number was settled to be two for both stable and transient soil variable sets in Kuresoi and Nyando.

~~As the analysis was purely exploratory, it was carried out as if we had little prior knowledge on the subject (i.e., we did not use the degradation states to guide the clustering analysis). We explored the results from three different clustering methods and used Rand index (Rand, 1971) to investigate the correspondence between the results. In this case, the Rand indices were moderate in the clustering of stable and transient variables. This suggested that the two clustering methods agreed to some extent. Finally, t-tests were applied to see if one clustering result separated the population better, and the results from the k-means clustering appeared to perform better in this case. Considering all the analyses and tests above, we chose to focus on discussing the clustering results from the k-means in the next section.~~
The k-means clustering analysis was implemented in R ~~using the "kmeans" function from base R~~ (R. Core Team, 2023) using ~~, and the and the "mclustBIC", "Mclust" functions from~~ the "mclust" package (Scrucca et al., 2023). ~~.~~ Investigation ~~Comparison~~ of the clustering results was carried out in R using ~~the "rand.index" function from~~ the "fossil" package (Vavrek, 2011).

Results

Relation of remote sensing classification to measured soil parameters

~~The results are presented as the letter-based display in brackets in Table 2. Boxplots of the variables with significant difference between degradation classes at p<0.1 level are shown in Figure 3~~Table 3 reports the mean and standard deviation for the soil variables measured in the two study areas and identifies those variables that~~which~~ showed significant differences between degradation states, which are then plotted in Figure 3. ~~From Table 2, we found that~~ Microbial biomass C and soil bulk density were the only two variables that showed significant differences ($p<0.1$) between degradation classes at both areas. ~~.~~ There was a significant increase ($p<0.05$) of 74% in mean microbial biomass C from degraded sites to ~~equilibrium~~ productive sites at Kuresoi, and a significant increase ($p<0.05$) of 70% at Nyando. Although the differences between the transition and degraded/~~equilibrium~~ productive sites were not significant, the rankings of the class means were consistent (degraded<transition<~~equilibrium~~productive) for both areas. The largest difference in soil bulk density was seen between the transition class and the ~~equilibrium~~ productive class for both Kuresoi ($p<0.05$) and Nyando ($p<0.05$). In this case, the rankings are inconsistent, with ~~equilibrium~~productive>degraded>transition at Kuresoi and transition>degraded>~~equilibrium~~ productive at Nyando, although the absolute differences between the classes were small (c.f. 0.1 g cm^3). Of the other soil variables that showed significant differences between degradation classes within each area~~,~~ ~~only~~

pH, total N and C and XYL at Kuresoi and C:N ratio at Nyando ranked the classes in the order degraded<transition<~~equilibrium~~productive; inorganic –P ranked the classes in the order of degraded > transition > productive, but the difference between degraded and transition is insignificant. Specifically~~:~~ at Kuresoi, mean pH increased by 0.4 from the degraded ~~class~~ to ~~equilibrium~~ productive class, mean total C increased from 6.1% to 7.9%, mean total N from 0.5% to 0.7%, and mean XYL increased by ~~approximately~~ 54%, from 172.9 to. 267.6 nmol h^{-1} g^{-1} dry soil. ~~;~~ A~~a~~t Nyando, soil C:N ratio increased from 12.1 in the degraded class to 13.2 in the ~~equilibrium~~ productive class.

Table 3.~~2~~ M~~Table of m~~ean and standard deviation (in brackets) of 28 soil variables (top 0-10 cm) by degradation labels measured at field sites in the two ~~locations~~study areas, Kuresoi and Nyando, along with the significance level of the between label differences from ANOVA (where * represents p < 0.1, and ** represents p < 0.05) . Variables that show a significant difference between degradation classes at the p<0.1 level as determined by a pairwise t-test are designated by a different letter in parenthesise.

Variable	Kuresoi				Nyando			
	Degraded	Transition	~~Equilibrium~~Productive	ANOVA	Degraded	Transition	~~Equilibrium~~Productive	ANOVA
Stable variables								
pH	5.0 ±0.5 (a) (n=19)	5.3±0.5 (b) (n=15)	5.4±0.5 (b) (n=11)	*	5.8±0.9 (n=10)	5.4±0.6 (n=14)	5.6±0.8 (n=20)	
Total inorganic N (mg kg^{-1})	21.7±14.8 (n=19)	21.0±13.4 (n=15)	31.7±18.9 (n=11)		9.9±7.0 (a) (n=11)	23.7±16.3 (b) (n=14)	13.6±6.7 (a) (n=19)	* *
Organic N (mg kg^{-1})	7.2±4.1 (n=19)	8.0±3.3 (n=15)	8.1±3.3 (n=11)		6.1±2.9 (a) (n=10)	9.3±3.6 (b) (n=14)	8.9±3.7 (b) (n=19)	*
Inorganic P (mg kg^{-1})	131.4±147.5 (n=19)	82.7±67.7 (n=15)	70.9±82.5 (n=11)		128.8±86.4 (ab) (n=11)	124.1±60.2 (a) (n=14)	90.4±68.7 (b) (n=20)	*
Total P (mg kg^{-1})	1093.4±568.3 (n=19)	1176.1±631.2 (n=15)	1328.2±729.3 (n=11)		660.2±421.5 (n=10)	457.0±188.0 (n=13)	523.3±367.9 (n=19)	
Total N (%)	0.5±0.1 (a) (n=19)	0.6±0.2 (ab) (n=15)	0.7±0.2 (b) (n=11)	*	0.2±0.1 (n=11)	0.3±0.1 (n=14)	0.3±0.1 (n=20)	
Total C (%)	6.1±1.7 (a) (n=19)	6.8±2.3 (ab) (n=15)	7.9±2.3 (b) (n=11)	*	2.8±1.3 (n=11)	4.1±1.4 (n=14)	3.8±1.9 (n=20)	
Soil bulk density (g cm-3)	0.8±0.1 (ab) (n=19)	0.7±0.1 (a~~ab~~) (n=15)	0.8±0.1 (b) (n=11)	* *	1.0±0.0 (a) (n=11)	1.1±0.1 (b) (n=14)	0.9±0.1 (c) (n=20)	* *
Aggregate stability Mean weigh	314.1±54.3 (n=18)	321.3±62.6 (n=15)	312.0±40.9 (n=10)		279.2±56.7 (n=5)	234.2±111.9 (n=11)	245.5±119.5 (n=17)	

t diameter (µm)							
Sand (%)	7.8±9.6 (n=18)	9.3±11.0 (n=15)	11.7±8.6 (n=10)		18.6±18.5 (n=10)	22.7±20.7 (n=13)	15.4±15.4 (n=20)	
Silt (%)	60.7±12.4 (n=18)	63.1±9.9 (n=15)	63.0±7.0 (n=10)		57.3±15.0 (ab) (n=10)	49.8±19.0 (a) (n=13)	65.0±12.5 (b) (n=20)	* *
Clay (%)	31.4±14.5 (n=18)	27.6±11.1 (n=15)	25.3±8.8 (n=10)		24.1±13.8 (n=10)	27.5±20.8 (n=13)	19.5±8.1 (n=20)	
CN ratio	12.0 ± 1.1 (n=19)	12.1 ± 0.8 (n=15)	11.5 ± 0.7 (n=11)		12.1 ± 1.2 (a) (n=11)	12.4 ± 1.3 (a) (n=14)	13.2 ± 0.8 (b) (n=20)	* *
CP ratio~~PHO (nmol h⁻¹ g⁻¹ dry soil)~~	76.8 ± 56.3 (n=19)~~3094.3±1130.5 (n=19)~~	74.6 ± 45.3 (n=15)~~3708.3±1236.4 (n=15)~~	120.1 ± 166.4 (n=11)~~3797.6±1408.5 (n=11)~~		83.9 ± 105.2 (n=10)~~1966.7±878.1 (n=11)~~	125.6 ± 109.7 (n=13)~~2701.1±1372.4 (n=14)~~	98.5 ± 62.1 (n=19)~~2160.2±1419.5 (n=20)~~	
NP ratio~~GLC (nmol h⁻¹ g⁻¹ dry soil)~~	6.5 ± 5.0 (n=19)~~200.0±131.4 (n=19)~~	6.1 ± 3.7 (n=15)~~221.2±117.4 (n=15)~~	10.4 ± 14.3 (n=11)~~269.4±122.4 (n=11)~~		7.3 ± 9.8 (n=10)~~229.3±104.7 (n=11)~~	10.5 ± 9.8 (n=13)~~349±226.625 (n=14)~~	7.6 ± 4.9 (n=19)~~230.6±231.6 (n=20)~~	
Transient variables								
N NAG (nmol h^{-1} g^{-1} dry soil)	82.2±41.0 (n=19)	99.3±56.5 (n=15)	83.4±44.4 (n=11)		78.4±45.5 (n=11)	97.7±40.3 (n=14)	72.5±30.2 (n=20)	
XYL (nmol h^{-1} g^{-1} dry soil)	172.9±92.6 (a) (n=19)	196.0±86.2 (ab) (n=15)	267.6±157.1 (b) (n=11)	*	197.8±86.9 (n=11)	259.2±166.5 (n=14)	175.2±148.9 (n=20)	
CBH (nmol h^{-1} g^{-1} dry soil)	34.3±11.0 (n=18)	42.7±14.6 (n=15)	41.9±23.6 (n=11)		33.5±27.2 (n=11)	36.4±26.0 (n=14)	44.4±47.2 (n=20)	
PER	11.1±14.4 (n=19)	8.9±8.5 (n=15)	6.9±7.4 (n=11)		4.1±3.0 (n=11)	3.2±1.9 (n=14)	4.8±2.6 (n=20)	

	(nmol h^{-1} g^{-1} dry soil)							
	POX (nmol h^{-1} g^{-1} dry soil)	0.3±0.2 (n=19)	0.3±0.3 (n=15)	0.2±0.2 (n=11)		0.3±0.1 (a) (n=11)	0.2±0.1 (b) (n=14)	0.3±0.1 (a) (n=20)	**
	URE (nmol h^{-1} g^{-1} dry soil)	8.7±5.7 (n=19)	6.9±6.1 (n=15)	10.5±6.8 (n=11)		8.0±7.5 (n=11)	12.3±8.9 (n=14)	7.3±5.8 (n=20)	
	KClNH$_4$ (mg kg^{-1})	9.5±17.5 (n=19)	8.1±7.4 (n=15)	9.3±13.7 (n=11)		7.0±4.6 (n=11)	9.4±9.3 (n=14)	8.5±7.0 (n=20)	
	$H_2ON O_3$ (mg kg^{-1})	13.3±14.4 (n=19)	12.3±11.5 (n=15)	22.4±18.8 (n=11)		3.9±4.9 (a) (n=11)	13.6±15.9 (b) (n=14)	7.8±17.8 (a) (n=20)	**
	Microbial C (mg kg^{-1})	1486.7±1171.9 (a) (n=19)	1760.0±1310.0 (ab) (n=15)	2583.0±1095.6 (b) (n=10)	*	863.6±568.0 (a) (n=11)	1167.7±618.6 (ab) (n=14)	1471.4±676.2 (b) (n=20)	**
	Microbial N (mg kg^{-1})	109.9±53.7 (n=15)	126.8±92.5 (n=15)	171.2±107.1 (n=9)		67.1±40.2 (n=11)	95.3±56.9 (n=14)	84.0±50.0 (n=18)	
	Dissolved Total C (mg kg^{-1})	267.7±73.2 (n=19)	296.3±85.7 (n=15)	288.1±96.5 (n=11)		293.3±95.9 (n=10)	319.3±82.4 (n=14)	338.8±152.2 (n=20)	
	Dissolved Organic C (mg kg^{-1})	263.7±73.3 (n=19)	293.3±86.8 (n=15)	283.4±93.5 (n=11)		269.0±83.3 (n=10)	301.5±71.7 (n=14)	322.6±145.1 (n=20)	
	Mineralisation (mg kg^{-1} d^{-1})	0.2±1.1 (n=19)	-0.0±0.8 (n=15)	-0.5±1.6 (n=10)		-0.2±1.0 (n=11)	-0.2±3.3 (n=14)	0.6±0.6 (n=20)	
	Nitrification	-0.1±1.1 (n=19)	-0.7±0.9 (n=15)	-1.2±1.7 (n=10)		-0.2±1.1 (n=11)	-0.1±2.7 (n=14)	-0.1±0.7 (n=20)	

(mg kg^{-1} d^{-1})							
CN ratio	12.0 ± 1.1 (n=19)	12.1 ± 0.8 (n=15)	11.5 ± 0.7 (n=11)	12.1 ± 1.2 (a) (n=11)	12.4 ± 1.3 (a) (n=14)	13.2 ± 0.8 (b) (n=20)	**
CP ratio	76.8 ± 56.3 (n=19)	74.6 ± 45.3 (n=15)	120.1 ± 166.4 (n=11)	83.9 ± 105.2 (n=10)	125.6 ± 109.7 (n=13)	98.5 ± 62.1 (n=19)	
NP ratio	6.5 ± 5.0 (n=19)	6.1 ± 3.7 (n=15)	10.4 ± 14.3 (n=11)	7.3 ± 9.8 (n=10)	10.5 ± 9.8 (n=13)	7.6 ± 4.9 (n=19)	

560

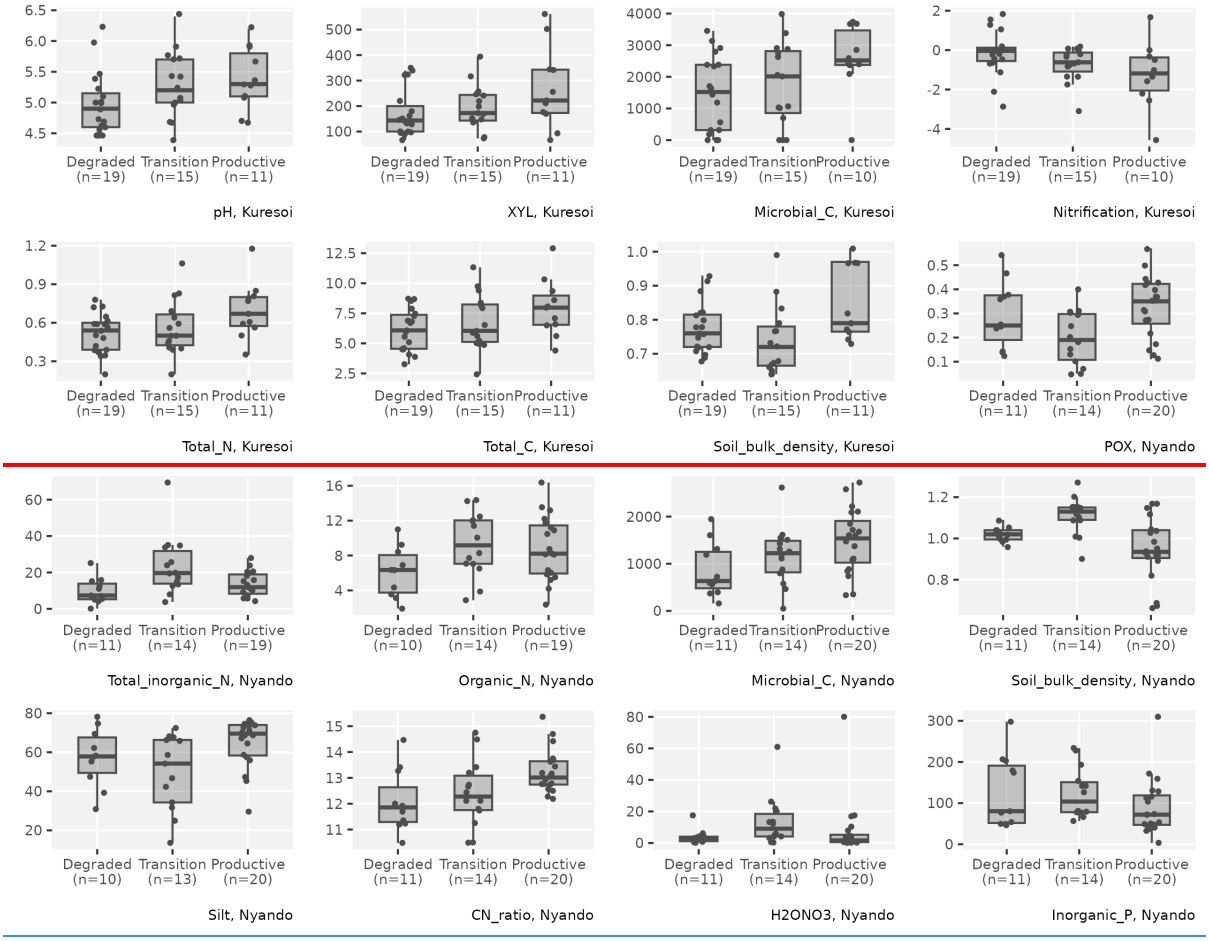
pH, Kuresoi
XYL, Kuresoi
Microbial_C, Kuresoi
Nitrification, Kuresoi
Total_N, Kuresoi
Total_C, Kuresoi
Soil_bulk_density, Kuresoi
POX, Nyando
Total_inorganic_N, Nyando
Organic_N, Nyando
Microbial_C, Nyando
Soil_bulk_density, Nyando
Silt, Nyando
CN_ratio, Nyando
H2ONO3, Nyando
Inorganic_P, Nyando
Degraded
Transition
Productive

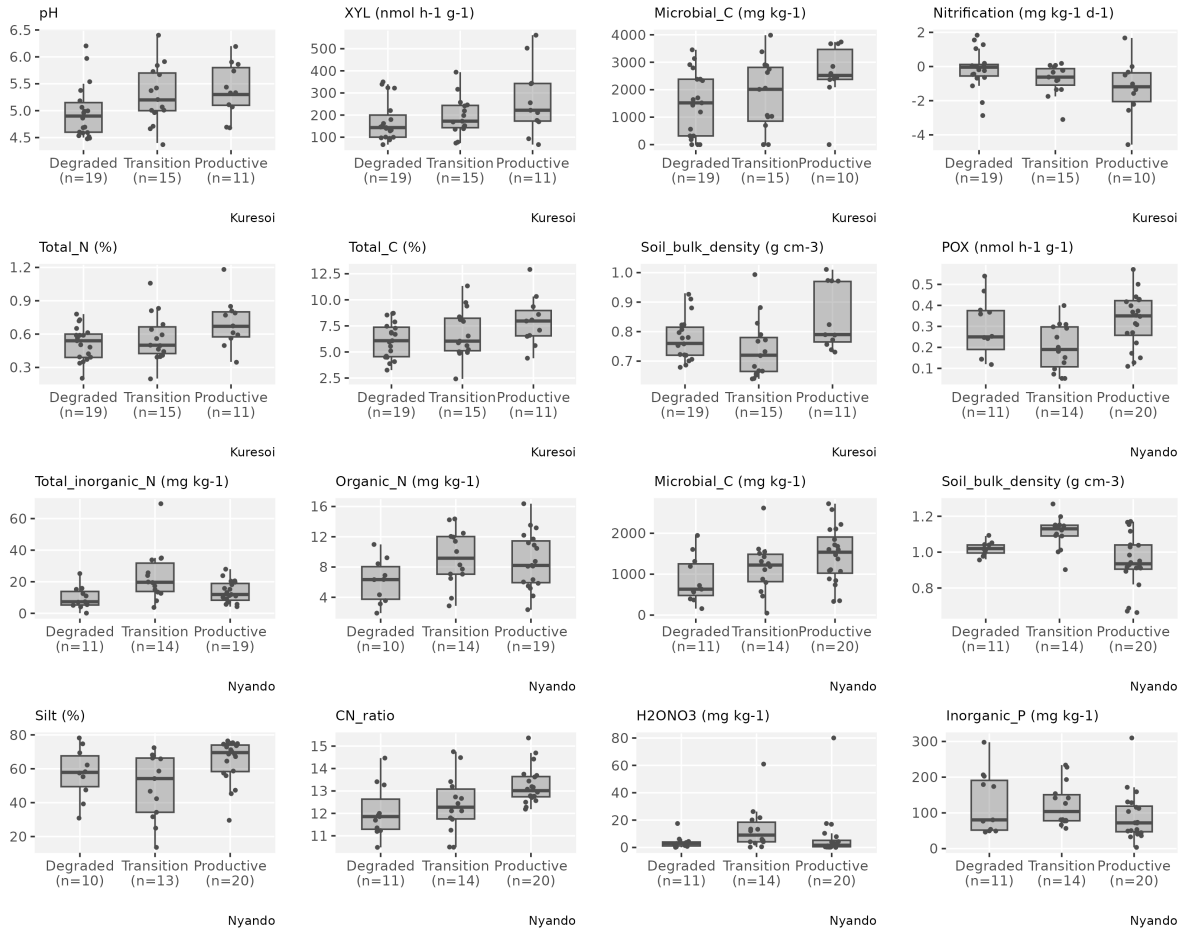

Figure 3: Box and whisker plots of the soil variables with significant difference between degradation classes based on ANOVA or Kruskal-Wallis test from Kuresoi and Nyando respectively. The dark grey dots are ~~the~~ observations overlaid on top of the box plots.

Which stable and transient soil variables explain the clustering of soils in the two study ~~sites~~areas?

Table ~~3~~45 summarises the number of sites in Kuresoi and Nyando that have been grouped into two clusters by the k-means algorithm for stable and transient variables. Note that the total number of sites used in ~~each~~ the clustering analysis ~~is~~ for each area is different.

Table 43: Number of sStabledegraded, transition and transient productive sites allotted to two clusters 1 and two at Kuresoi and Nyando using K-means clustering for stable and transient variables..

	Kuresoi		Nyando	
	Cluster 1	Cluster 2	Cluster 1	Cluster 2
Stable variables				
Degraded	8	9	2	3
Transition	8	7	4	6
Productive	2	7	4	12
Total	18	23	10	21
Transient variables				
Degraded	4	10	2	8
Transition	6	9	8	6
Productive	6	3	5	13
Total	16	22	15	27

	Kuresoi		Nyando	
	Cluster 1	Cluster 2	Cluster 1	Cluster 2
Stable	18	23	10	21
Transient	16	22	15	27

For the stable variables, in Kuresoi, sites in cluster 2 had significantly higher values of total N, total inorganic N, organic N, total P, total C and pH (significant atp-value < 0.05 level under two-sample t-tests). There was a significant difference in silt and clay contents of the two clusters. From Table 4,3, wWe seefound that 7 out of 9 Kuresoi equilibrium productive sites, from the remote sensing classification, were assigned to this cluster 2, but the numbers of transitional and degraded sites were distributed evenly between two clusters. Similarly, in Nyando, one cluster (cCluster 2) tended to hadve higher levels of total P, total N and total C, but lower pH and relatively low soil bulk density (all significant at p<0.05 level). There was a significant difference in sand, silt and clay percentages. In total, 12 out of 16 equilibrium productive sites in Nyando were assigned to this cluster. The transitional and degraded sites appeared to be equally likely in two clusters. Density plots showing how the two clusters differ in selected stable variables are given in the top five panels in Figures 3 (Kuresoi) and 4 (Nyando). For the transient variables, in Kuresoi, sites in one cluster (cCluster 1) tended to have higher PHO, GLC, XYL, CBH, but lower POX. It also had higher microbial N, nitrate (extracted in H_2O NO_3), microbial C, total dissolved C. In Nyando, one cluster (cCluster 1) consisted of sites with higher PHO, GLC, XYL, NAG, total dissolved C, but lower PER and POX. The cluster labels did not match the degradation labels in both cases. This is not surprising as the transient variables are highly variable and can change substantially in a short period of time. Density Box plots showing how the two clusters differedd in selected stable (Figure 4) and transient (Figure 5) variables are given in the bottom panels of Figures *3 (for Kuresoi) and 4 * (Nyando). All variables shown in the figures have significant mean difference at p<0.05 level under a two-sample t-test.

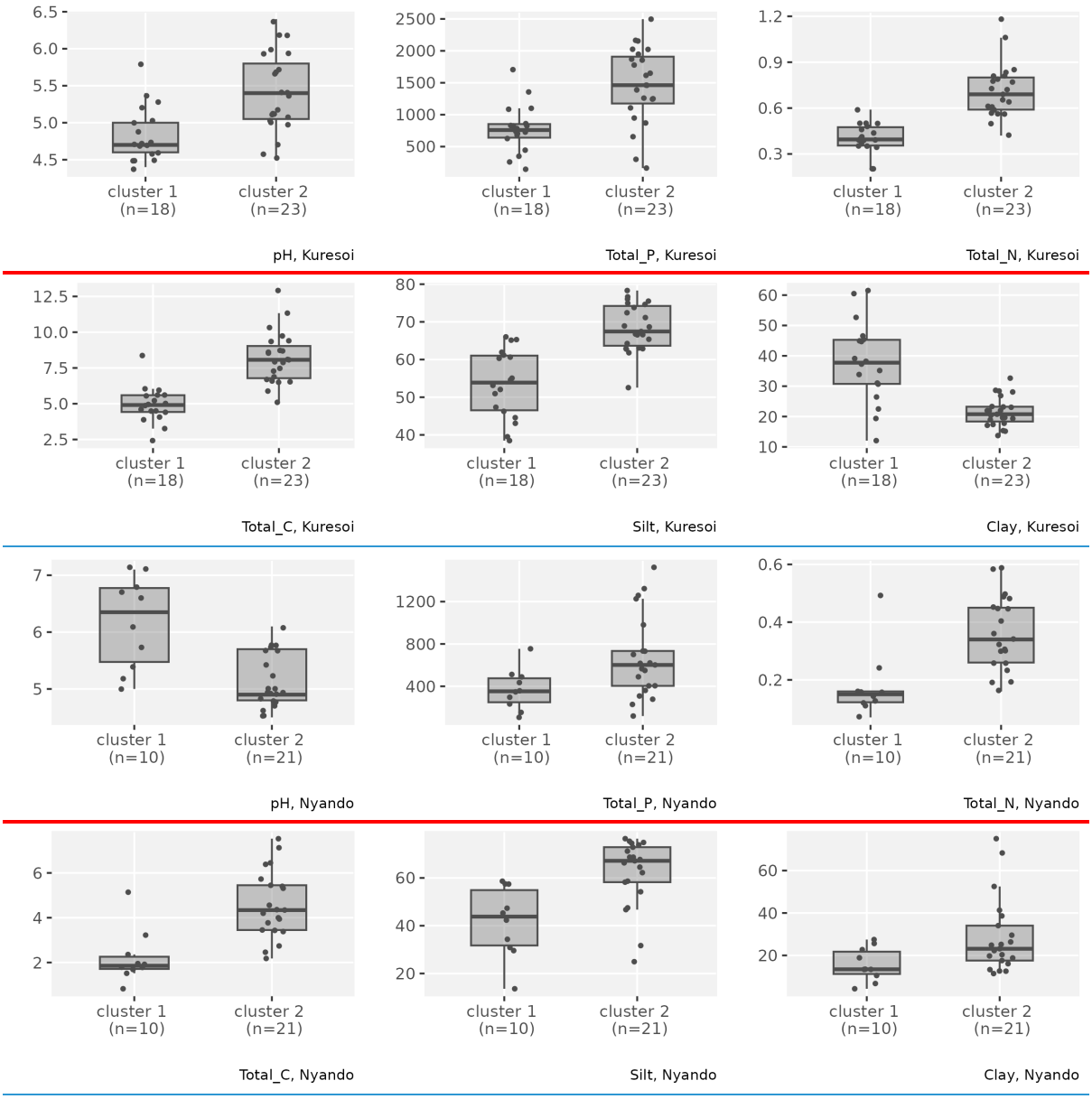
6.5
6.0
5.5
5.0
4.5
cluster 1 (n=18)
cluster 2 (n=23)
pH, Kuresoi
2500
2000
1500
1000
500
cluster 1 (n=18)
cluster 2 (n=23)
Total_P, Kuresoi
1.2
0.9
0.6
0.3
cluster 1 (n=18)
cluster 2 (n=23)
Total_N, Kuresoi
12.5
10.0
7.5
5.0
2.5
cluster 1 (n=18)
cluster 2 (n=23)
Total_C, Kuresoi
80
70
60
50
40
cluster 1 (n=18)
cluster 2 (n=23)
Silt, Kuresoi
60
50
40
30
20
10
cluster 1 (n=18)
cluster 2 (n=23)
Clay, Kuresoi
7
6
5
cluster 1 (n=10)
cluster 2 (n=21)
pH, Nyando
1200
800
400
cluster 1 (n=10)
cluster 2 (n=21)
Total_P, Nyando
0.6
0.4
0.2
cluster 1 (n=10)
cluster 2 (n=21)
Total_N, Nyando
6
4
2
cluster 1 (n=10)
cluster 2 (n=21)
Total_C, Nyando
60
40
20
cluster 1 (n=10)
cluster 2 (n=21)
Silt, Nyando
60
40
20
cluster 1 (n=10)
cluster 2 (n=21)
Clay, Nyando

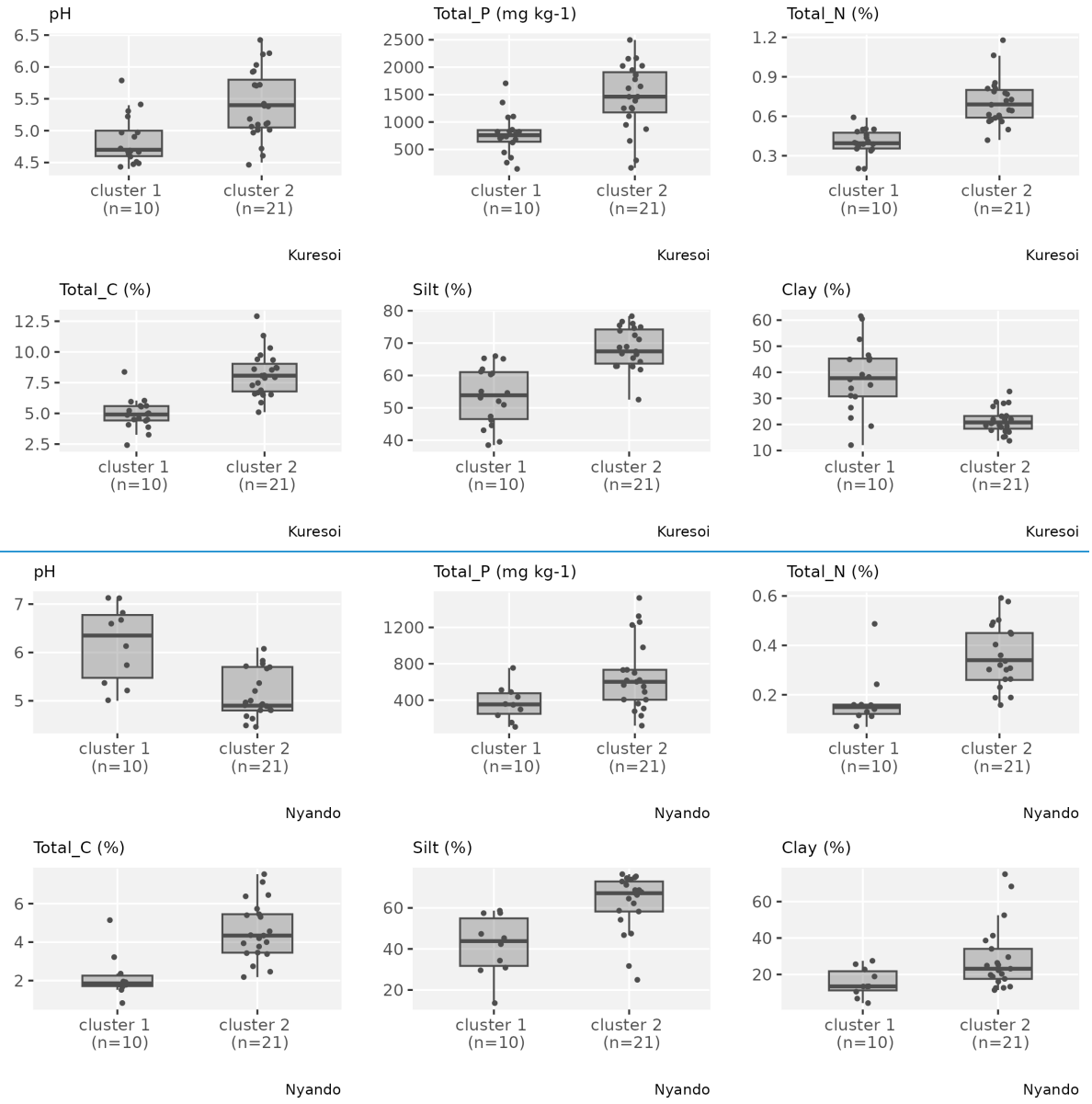

Figure 4: Box and whisker plots of selected stable variables that show a significant mean difference ($p<0.05$) between two clusters in both Kuresoi and Nyando, with observations (grey dots) overlaid on top.

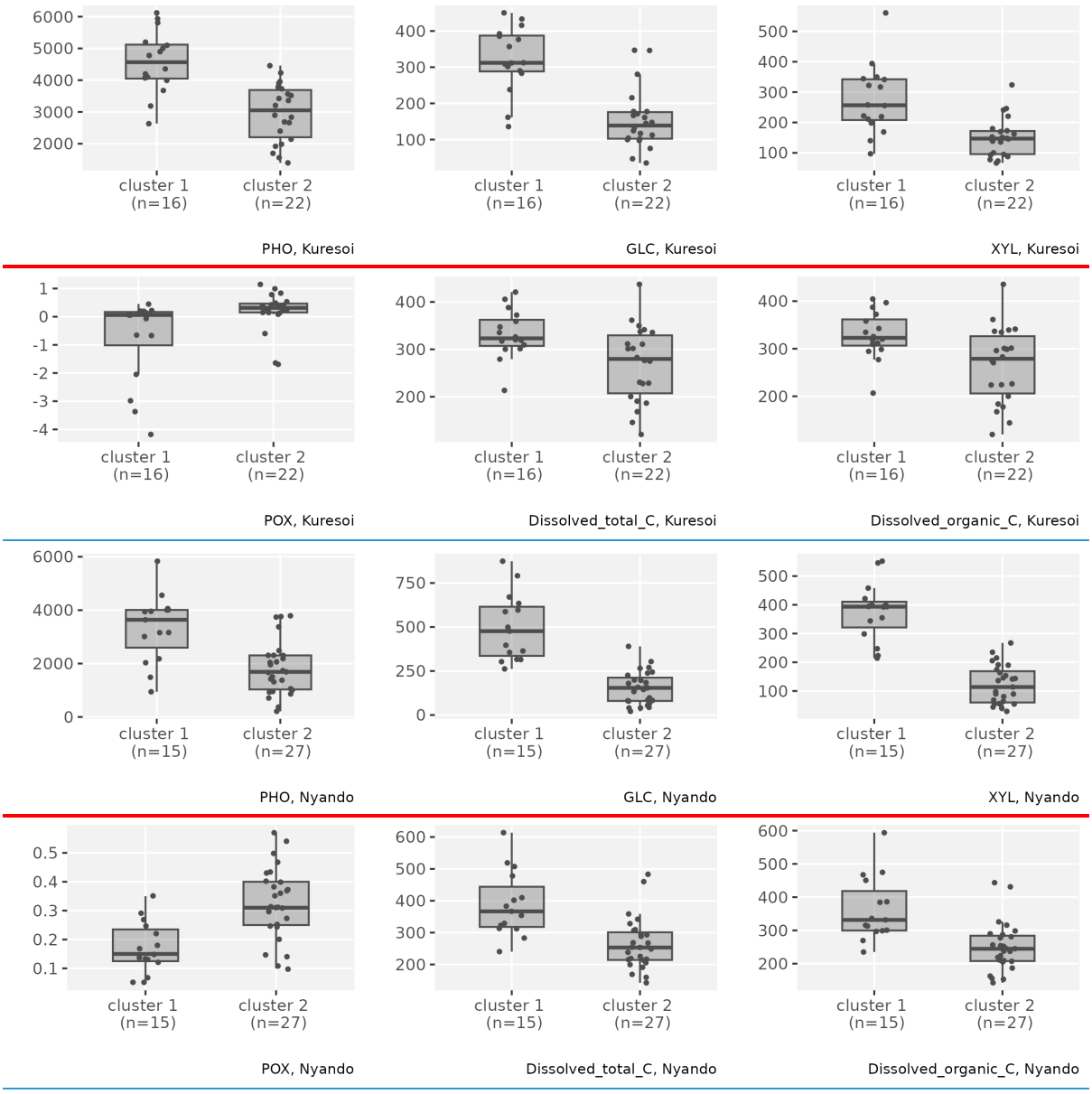
6000
5000
4000
3000
2000
cluster 1 (n=16)
cluster 2 (n=22)
PHO, Kuresoi
400
300
200
100
GLC, Kuresoi
500
400
300
200
100
XYL, Kuresoi
1
0
-1
-2
-3
-4
POX, Kuresoi
Dissolved_total_C, Kuresoi
Dissolved_organic_C, Kuresoi
6000
4000
2000
0
cluster 1 (n=15)
cluster 2 (n=27)
PHO, Nyando
750
500
250
GLC, Nyando
XYL, Nyando
0.5
0.4
0.3
0.2
0.1
POX, Nyando
600
Dissolved_total_C, Nyando
Dissolved_organic_C, Nyando

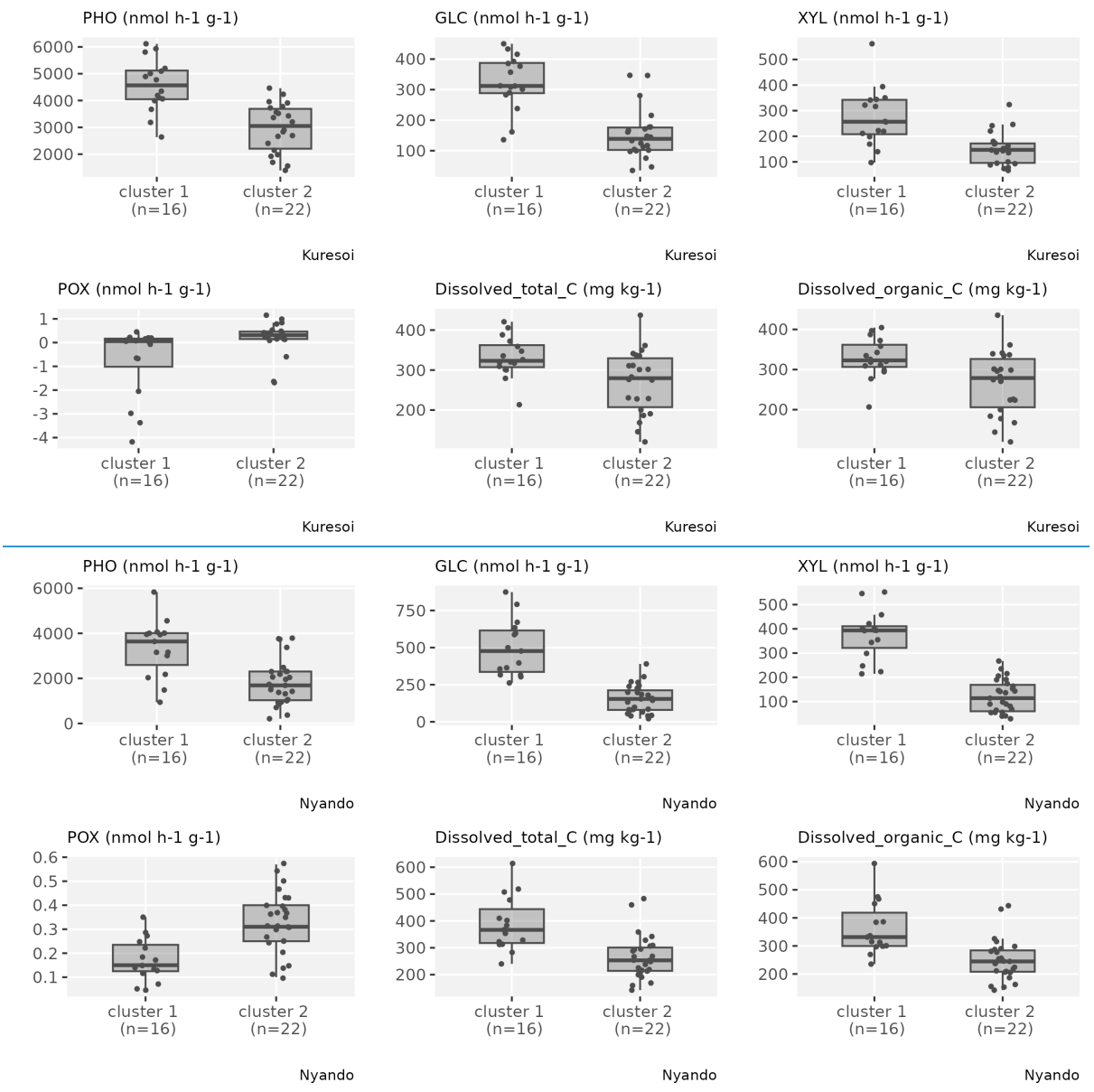

Figure 5: Box and whisker plots of selected transient variables that show a significant mean difference ($p<0.05$) between two clusters in both Kuresoi and Nyando, with observations (grey dots) overlaid on top.

To further investigate the features of the clusters, we evaluated the inter-quantile range (IQR) between the 0.15 and 0.85 quantiles of the samples from sites allocated to each cluster, representing the spread of about 70% of the samples. For stable variables in Kuresoi, the IQRs of the samples from sites allocated to cluster 1 are 401 to 1091 (mg kg^{-1}) for total P, 0.35~~45~~% to 0.50~~0~~% for total N, and 3.984% and 5.76~~3~~% for total C. Whereas the IQRs of the sites allocated to cluster 2 are 893 to 2024 (mg kg^{-1}) for total P, 0.56~~3~~% to 0.824% for total N, and 6.55~~48~~% and 9.64~~38~~% for total C. In Nyando, the sites allocated to cluster 1 have IQRs of 181 to 503 (mg kg^{-1}) for total P, 0.11~~3~~% to 0.21~~2~~% for total N and 1.58~~79~~% to 2.92~~19~~% for total C. The sites allocated to cluster 2 have IQRs of 307 to 1226 (mg kg^{-1}) for total P, 0.23~~0~~% to 0.49~~0~~% for total N and 3.38~~0~~%

to 6.380% for total C. Overall, the clustering analysis grouped the sites with higher or lower total N and total C relatively well, with the IQRs show clear difference between two clusters. However, there are some overlaps between the IQRs of total P from two clusters for both Kuresoi and Nyando. For the transient variables, we see mostly overlapping IQRs between clusters, with the exception of GLC in Kuresoi, and GLC, XYL in Nyando.

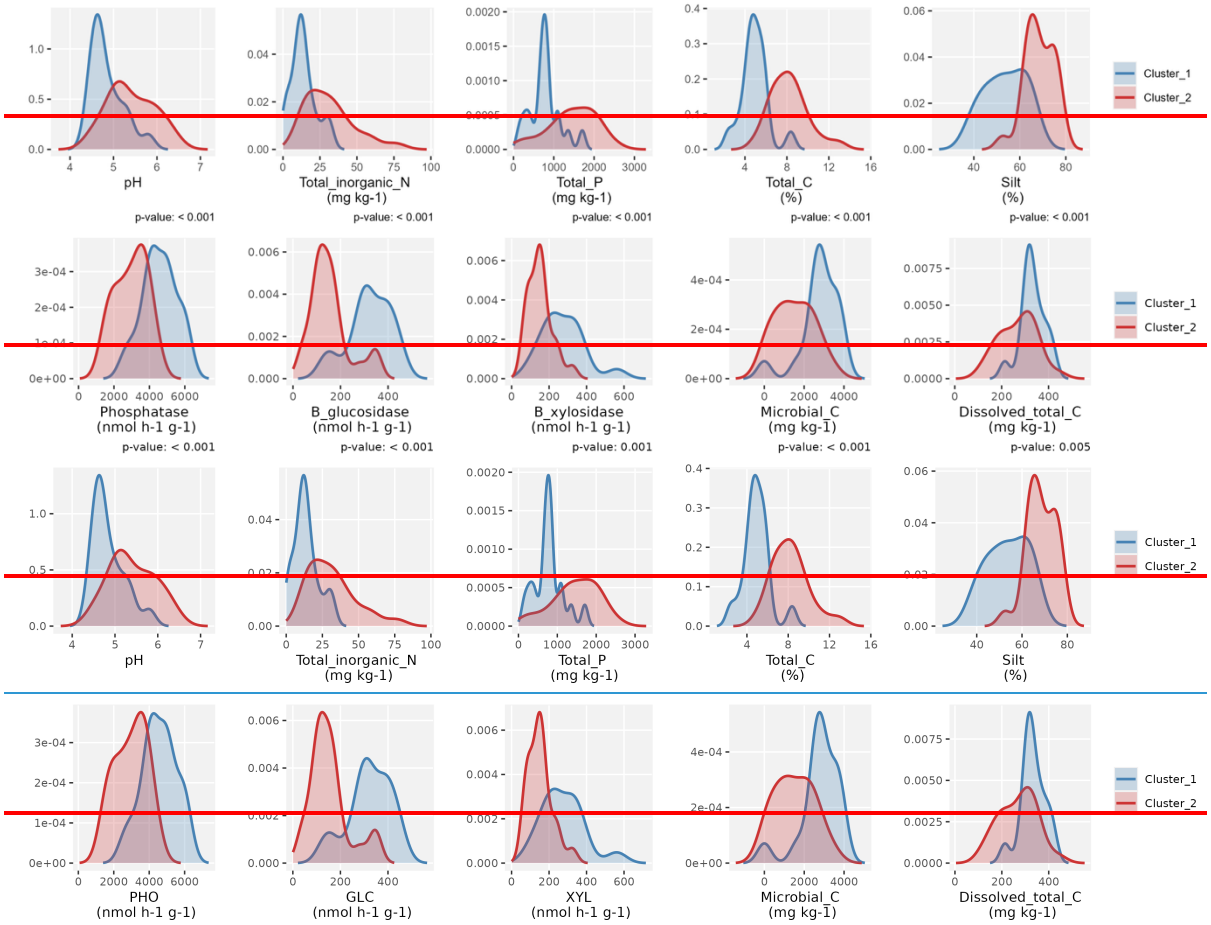

Figure S*3. Density plots of selected stable variables from sites that are grouped into two clusters (top panels) and transient variables from sites that are grouped into two clusters (bottom panels) in Kuresoi.

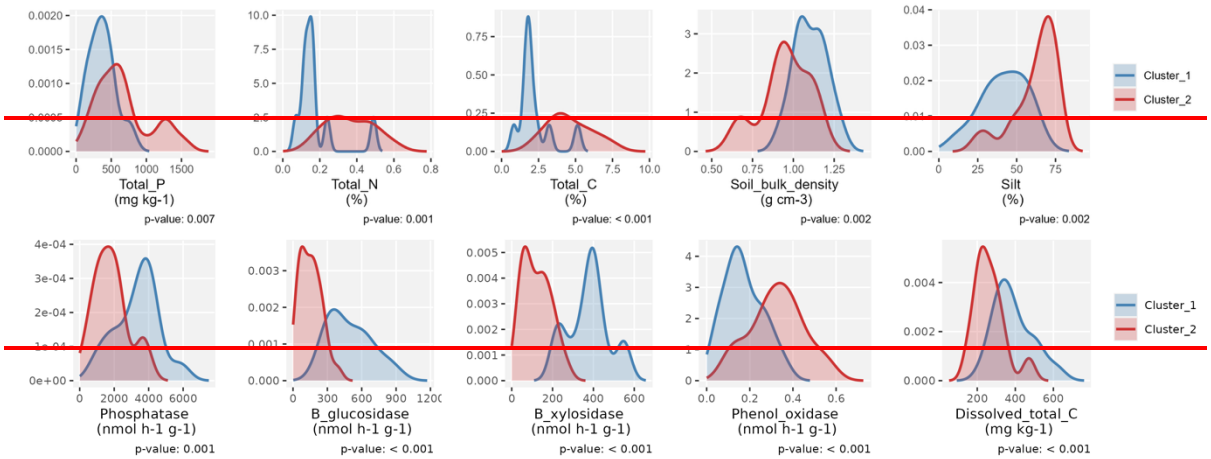

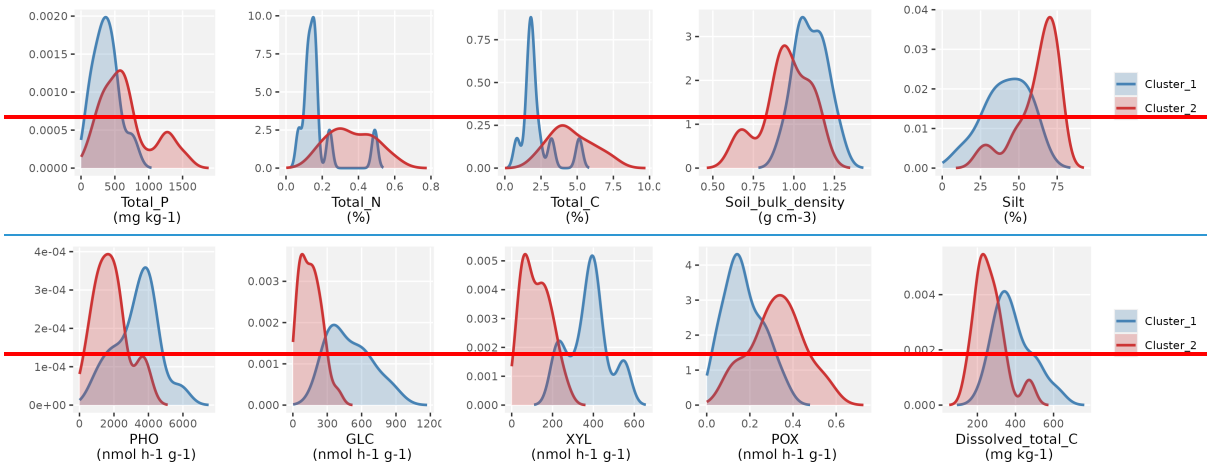

~~Figure S*4. Density plots of selected stable variables from sites that are grouped into two clusters (top panels) and transient variables from sites that are grouped into two clusters (bottom panels) in Nyando.~~

Discussion

~~Remote sensing is a powerful tool to assess soil degradation and has been utilised globally in many studies (e.g. Cordell et al., 2017; Manić et al., 2022; Wang et al., 2024)~~ The ability of remote sensing to classify degradation status over large areas (e.g. Cordell et al., 2017; Manić et al., 2022; Wang et al., 2024), at relatively low cost and utilising data that can be rapidly updated as new images become available, is an attractive proposition, since it provides land managers, policy makers and scientists with a mechanism for targeting interventions. Combined remote sensing and measurement of soil properties has been used to ~~Soil m~~map ~~ping of~~ soils ~~properties and soil degradation has combined remote sensing and measured soil properties to map soils~~ in Africa with some success (Vågen et al., 2016). Nevertheless, there have been relatively few attempts to compare remotely sensed classification against soil data collected from soil sampling programmes. Our work demonstrates that, while it is relatively straightforward to generate classifications using derived parameters, such as NDVI, NDWI and EVI, that reflect vegetation dynamics, the resulting classification ~~poorly~~ only reflected~~s~~ changes in ~~multiple~~ a few in-situ soil parameters related to soil degradation.

~~However, a~~Across the two studied districts (i.e., Nyando and Kuresoi) we detected consistent alignment between remote sensing classification of degradation and microbial biomass C, a key soil biological parameter related to nutrient and C cycling processes in soil (Tate, 2017) that is tightly linked to plant diversity and productivity (Chen et al., 2019) and is known to respond quickly (c.100 days) to inputs of fresh organic matter to soil, including plant litter and animal wastes (Dai et al., 2021b). Therefore, it is likely that we are seeing the soil response to the amount of litter, root exudates, and dung from grazing animals, that is returned to the soil, all of which are functions of above-ground biomass reflected in the dynamics of NDVI.

Apart from microbial biomass C, only bulk density showed differences ~~at both sites~~related to degradation ~~at~~in both ~~sites~~study areas, although ~~but in its case,~~ the rankings were inconsistent and inter-site differences small. T~~t~~here was little consistent agreement between the remotely sensed classification with other field-based soil variables (Table 2). ~~–~~ Some variables considered good proxy indicators for soil health and which correlate~~d~~ with other important soil functions (Lal, 2016), such as C and N concentrations~~Some variables related to soil degradation, such as C and N concentrations~~, C:N ratio and pH, were statistically significant for one site, but not the

other. ~~. Soil C and N concentrations are considered good proxy indicators for soil health and are correlated with other important soil functions (Lal, 2016), and they were lower in degraded soils in Burkina Faso compared to those under native vegetation (Traoré et al., 2015). However, in our study all sampled sites are managed grasslands, providing less of a contrast.~~

We see two problems with the use of RS classification of soil degradation in the western Kenyan environment. First~~ly An additional problem with the RS classification~~ is the difficulty associated with unravelling the effect of rainfall variability and soil degradation as observed remotely (Wessels et al., 2007), whereby it may be difficult to distinguish the role of drought and degradation. These difficulties are compounded in the context of smallholder farming due to grazing occurring on small parcels of land where plant biomass is variable and depends not only on soil and rainfall, but upon frequency and intensity of grazing. Thus, in these situations, counter-intuitive results are possible. For example, following a drought it is likely that grazing takes place on the most resilient and rapidly recovering areas ~~,(~~ the ~~equilibrium~~ productive and transitional ~~plots~~ sites in this study)~~,~~ rather than those that are slow to revegetate (the degraded sites), potentially resulting in misclassification of ~~equilibrium~~ productive conditions as degraded ~~with RS vegetation indices~~. Second~~ly~~, as the RS was used to plan the soil survey, it meant that the RS images did not coincide with the survey dates. However, given that we ~~are~~ used~~ing the~~ RS data to consider seasonal shifts in vegetation indices over six years (Table 1), we do not think that an additional year of data would have changed our findings.

~~Using a statistical approach to classifying the sites without the guidance of the RS degradation labels, the plots were grouped into two distinct clusters. These were distinguished based on stable soil properties which would be expected to be associated with good soil health, such as total C, N, P and pH.~~ The clustering had~~s~~ some overlap with the ~~equilibrium~~ productive ~~plots~~ sites in both ~~sites~~ areas and therefore provides an indication of a reduced number of soil properties that could be used to guide targeting efforts for restoration. The cluster analysis revealed some consistent patterns within the soil data and some agreement between the clustering and the classification derived from remote sensing with seven out of nine and 12 out of 16 ~~equilibrium~~ productive sites attributed to the same cluster at Kuresoi and Nyando, respectively. These ~~'~~higher ~~equilibrium~~nutrient status~~'~~ clusters were characterised by higher soil N, P and C contents ~~at~~ in both ~~sites~~study areas, suggesting that these clusters are more fertile. This was supported by the separation between the inter-quantile ranges for total N and total P in both study areas. pH was also an important variable in the two clusters ~~at~~ in both ~~sites~~study areas, but with lower pHs featuring in the Nyando study ~~site~~ area and higher pHs at Kuresoi. This reflects the different soils present in the two areas: soils at Nyando are prone to salinisation and tend to have a higher overall pH compared to the more acidic soils at Kuresoi, so it appears that what we are seeing in the '~~equilibrium~~productive' clusters is the inclusion of more favourable, slightly acid pHs ~~at both sites~~in both study areas. Of the transient variables, the enzymes PHO, GLC and XYL featured in the ~~'equilibrium~~higher nutrient status~~'~~ clusters ~~at~~ in both ~~sites~~study areas. Both GLC and XYL are key for breaking down cellulose and releasing energy for the soil microbial community, while PHO plays an important role in releasing P from organic matter for plant uptake (Jackson et al., 2013). ~~Their presence here could indicate that C and P are more limiting in the 'equilibrium' cluster., however, there is a lack of corroboration for this in the macronutrient data with C:N, C:P and N:P ratios showing no significant difference (p <0. 5) between clusters at either site.~~

Our data ~~set~~, although extensive in terms of soil chemical and biological parameters~~stry, , soil biology~~ only considered one soil physical variable, aggregate stability, and thus provides ~~only~~ limited insights into the physical condition of the soils. It is possible that the inclusion of infiltration rates and water holding capacity into our measurements may have produced a better relationship between RS and soil properties related to degradation. Work in China ~~(Yi et al., 2012)~~ demonstrated a reduction in water holding capacity with increasing levels of degradation classified using grassland species composition (Yi et al., 2012), and ~~in a second study (Zeng et al., 2013)~~ hydraulic conductivity was shown to decline~~d~~ with~~as~~ degradation, defined by vegetation parameters (Zeng et al., 2013). However, more recent studies, using shrub coverage as the basis for degradation classification, report less clear relationships between soil water parameters and degradation (Dai et al., 2021a). ~~Our work points to the need to combine remote sensing techniques with field surveys, but with a reduced set of measurements. Remote sensing is a powerful tool and provides a cost-effective methodology for soil degradation assessment at ever increasing resolution, but it is prone to error. This is particularly the case in landscapes with highly heterogeneous smallholder grazing lands, such as those in Nyando and Kuresoi, where vegetation cover and greenness, may be affected by intense grazing pressure resulting in the misclassification of some sites, as shown in our work.~~
(Dai et al., 2021a; Yi et al., 2012; Zeng et al., 2013)~~On the other hand, field-work is expensive and requires laboratory support, which is also costly and not always available in SSA. However, our work demonstrates that utilising a relatively small set of soil variables (soil microbial C, total C and Total N) can provide additional support for classifications derived from remote sensing.~~

Conclusion

Remote sensing was able to map grassland degradation over large areas of western Kenya and offers the potential for cost-effective and dynamic monitoring. However, when the RS classification was compared to measured soil variables, apart from microbial C, soil C and N in one or other of the study areas, agreement was generally poor. This is probably due to the highly heterogeneous smallholder grazing land~~s~~e in Nyando and Kuresoi. Here, vegetation cover and greenness~~,~~ is affected by variations in livestock ~~intense~~ grazing pressure as well as soil degradation status, resulting in only limited agreement with measured soil values~~However, it aligned only with a small subset of soil parameters, with soil microbial C being the only parameter which consistently reflected changes in the degradation classes identified from RS in both Nyando and Kuresoi. Additionally, some soil variables reflecting soil C and N status did relate to the degradation classes at one or the other site. We expect that variability in livestock grazing patterns and local climatic differences may have led to some of the miss-classifications by RS.~~

The statistical clustering produced two clusters in~~at~~ each of the ~~sites~~ areas based on stable and transient or dynamic soil properties. The clusters ~~at~~ for each of the ~~sites~~ study areas largely reflected differences in nutrient status and biogeochemical cycling, ~~particularly~~with one cluster at in each area having higher ~~values of total~~ soil N, ~~total~~ P, and~~Total and~~ C contents~~,~~ and greater activities of selected extracellular enzymes (i.e., ~~contents and~~ PHO, GLC and XYL) ~~concentrations~~;~~,~~ ~~with~~ seven out of nine and 12 out of 16 ~~equilibrium~~ productive sites attributed to this ~~the same~~ cluster at Kuresoi and

Nyando, respectively. In addition, separation between the inter-quantile ranges between the clusters in both study areas was found for total soil N and ~~total~~ C. Thus, when assessing soil degradation in grazed smallholder farming settings we propose ~~Our research demonstrates the potential power of RS approaches to the assessment of soil degradation, allowing temporally and spatial patterns of degradation to be resolved, but also suggests that~~ sampling a small additional set of soil variables that pertain to biogeochemical cycling (soil microbial C, total C and t~~T~~otal N) ~~can provide additional support for the classification~~ to provide confidence for~~,~~ identifying degraded soils and helping to target restoration efforts~~.~~.

Author contributions

JQ and MR led the writing of the paper, MR led the study and secured the funding for the work, along with RDB, JH and JQ. All authors contributed to the manuscript. In addition, GY and GB carried out the remote sensing analysis and contributed to the data analysis, MG carried out data analysis, KK, EF, YO, BN PDB, AO collected field data.

Acknowledgements

We acknowledge funding from the UK Biotechnology and the Biological Sciences Research Council (UKRI-BBSRC), through the Global Challenges Research Fund (GCRF) under Agri-systems research to enhance rural livelihoods in developing countries [grant number BB/S014934/1]. SML and KK acknowledge the CGIAR trust fund for funding received through the Science Programmes Climate Action, Multifunctional Landscapes, and Sustainable Farming.

Dedication

We dedicate this paper to Mariana Rufino and Joseph Hitimana, committed scientists and educator~~,~~s and critical to the success of this work who sadly both died before this paper could be published.

References

Arias-Navarro, C., Díaz-Pinés, E., Zuazo, P., Rufino, M. C., Verchot, L. V., and Butterbach-Bahl, K.: Quantifying the contribution of land use to N 2 O, NO and CO 2 fluxes in a montane forest ecosystem of Kenya, Biogeochemistry, 134, 95-114, 2017.

Augustine, D. J., McNaughton, S. J., and Frank, D. A.: Feedbacks between soil nutrients and large herbivores in a managed savanna ecosystem, Ecological Applications, 13, 1325-1337, 2003.

Bai, Y. and Cotrufo, M. F.: Grassland soil carbon sequestration: Current understanding, challenges, and solutions, Science, 377, 603-608, 2022.

Barbier, E. B. and Hochard, J. P.: Does land degradation increase poverty in developing countries?, PloS one, 11, e0152973, 2016.

Bardgett, R. D., Bullock, J. M., Lavorel, S., Manning, P., Schaffner, U., Ostle, N., Chomel, M., Durigan, G., L Fry, E., and Johnson, D.: Combatting global grassland degradation, Nature Reviews Earth & Environment, 2, 720-735, 2021.

Berisso, F. E., Schjønning, P., Keller, T., Lamandé, M., Etana, A., de Jonge, L. W., Iversen, B. V., Arvidsson, J., and Forkman, J.: Persistent effects of subsoil compaction on pore size distribution and gas transport in a loamy soil, Soil and Tillage Research, 122, 42-51, https://doi.org/10.1016/j.still.2012.02.005, 2012.

Brandt, M., Wigneron, J.-P., Chave, J., Tagesson, T., Penuelas, J., Ciais, P., Rasmussen, K., Tian, F., Mbow, C., and Al-Yaari, A.: Satellite passive microwaves reveal recent climate-

induced carbon losses in African drylands, Nature ecology & evolution, 2, 827-835, 2018.
Bridges, E. and Oldeman, L.: Global assessment of human-induced soil degradation, Arid soil research and rehabilitation, 13, 319-325, 1999.
Broadbent, A. A., Bahn, M., Pritchard, W. J., Newbold, L. K., Goodall, T., Guinta, A., Snell, H. S., Cordero, I., Michas, A., and Grant, H. K.: Shrub expansion modulates belowground impacts of changing snow conditions in alpine grasslands, Ecology Letters, 25, 52-64, 2022.
Chen, C., Chen, H. Y. H., Chen, X., and Huang, Z.: Meta-analysis shows positive effects of plant diversity on microbial biomass and respiration, Nature Communications, 10, 1332, 10.1038/s41467-019-09258-y, 2019.
Cordell, S., Questad, E. J., Asner, G. P., Kinney, K. M., Thaxton, J. M., Uowolo, A., Brooks, S., and Chynoweth, M. W.: Remote sensing for restoration planning: how the big picture can inform stakeholders, Restoration Ecology, 25, S147-S154, https://doi.org/10.1111/rec.12448, 2017.
Cordero, I., Leizeaga, A., Hicks, L. C., Rousk, J., and Bardgett, R. D.: High intensity perturbations induce an abrupt shift in soil microbial state, The ISME Journal, 17, 2190-2199, 10.1038/s41396-023-01512-y, 2023.
Dai, L., Guo, X., Ke, X., Du, Y., Zhang, F., and Cao, G.: The variation in soil water retention of alpine shrub meadow under different degrees of degradation on northeastern Qinghai-Tibetan plateau, Plant and Soil, 458, 231-244, 10.1007/s11104-020-04522-3, 2021a.
Dai, W., Peng, B., Liu, J., Wang, C., Wang, X., Jiang, P., and Bai, E.: Four years of litter input manipulation changes soil microbial characteristics in a temperate mixed forest, Biogeochemistry, 154, 371-383, 10.1007/s10533-021-00792-w, 2021b.
Eckert, S., Hüsler, F., Liniger, H., and Hodel, E.: Trend analysis of MODIS NDVI time series for detecting land degradation and regeneration in Mongolia, Journal of Arid Environments, 113, 16-28, 2015.
Eklundh, L. and Jönsson, P.: TIMESAT: A software package for time-series processing and assessment of vegetation dynamics, in: Remote Sensing Time Series, Springer, 141-158, 2015.
Eklundh, L. and Jönsson, P.: TIMESAT 3.3 software manual, Lund and Malmö University, Lund, Sweden, 2017.
Ellis, J. E. and Swift, D. M.: Stability of African Pastoral Ecosystems: Alternate Paradigms and Implications for Development, J. Range Manage., 41, 450-459, 10.2307/3899515, 1988.
Fraley, C. and Raftery, A. E.: Model-Based Clustering, Discriminant Analysis, and Density Estimation, Journal of the American Statistical Association, 97, 611-631, 2002.
Gibbs, H. K. and Salmon, J. M.: Mapping the world's degraded lands, Applied Geography, 57, 12-21, http://dx.doi.org/10.1016/j.apgeog.2014.11.024, 2015.
Hartigan, J. A. and Wong, M. A.: Algorithm AS 136: A K-Means Clustering Algorithm, Journal of the Royal Statistical Society. Series C (Applied Statistics), 28, 100-108, 1979.
He, M., Kimball, S. J., Maneta, P. M., Maxwell, D. B., Moreno, A., Beguería, S., and Wu, X.: Regional Crop Gross Primary Productivity and Yield Estimation Using Fused Landsat-MODIS Data, Remote Sensing, 10, 2018.
Huete, A. R., HuiQing, L., and Leeuwen, W. J. D. v.: The use of vegetation indices in forested regions: issues of linearity and saturation, IGARSS'97. 1997 IEEE International Geoscience and Remote Sensing Symposium Proceedings. Remote Sensing - A Scientific Vision for Sustainable Development, 1966-1968,

Hulett, J. L., Weiss, R. E., Bwibo, N. O., Galal, O. M., Drorbaugh, N., and Neumann, C. G.: Animal source foods have a positive impact on the primary school test scores of Kenyan schoolchildren in a cluster-randomised, controlled feeding intervention trial, The British Journal of Nutrition, 111, 875–886, 2014.
IUSS: World reference base for soil resources 2014. Update 2015. International soil classification system for naming soils and creating legends for soil maps. World Soil Resources Reports No. 106, FAO, Rome2015.
Jackson, C. R., Tyler, H. L., and Millar, J. J.: Determination of Microbial Extracellular Enzyme Activity in Waters, Soils, and Sediments using High Throughput Microplate Assays, Journal of Visualized Experiments : JoVE, 80, 10.3791/50399, 2013.
Jacobs, S. R., Breuer, L., Butterbach-Bahl, K., Pelster, D. E., and Rufino, M. C.: Land use affects total dissolved nitrogen and nitrate concentrations in tropical montane streams in Kenya, Science of The Total Environment, 603-604, 519-532, https://doi.org/10.1016/j.scitotenv.2017.06.100, 2017.
Jennings, D. J.: Geology of the Molo area (No. 86). 1971.
Johnson, R. A. and Wichern, D. W.: Applied Multivariate Statistical Analysis, Pearson Prentice Hall, U.S.2007.
Kemper, W. D. and Koch, E. J.: Aggregate stability of soils from Western United States and Canada: Measurement procedure, correlations with soil constituents, 1355, Agricultural Research Service, US Department of Agriculture1966.
Kjeldahl, J.: Neue Methode zur Bestimmung des Stickstoffs in organischen Körpern, Zeitschrift für analytische Chemie, 22, 366-382, 10.1007/BF01338151, 1883.
Kong, D., McVicar, T. R., Xiao, M., Zhang, Y., Peña-Arancibia, J. L., Filippa, G., Xie, Y., and Gu, X.: phenofit: An R package for extracting vegetation phenology from time series remote sensing, Methods in Ecology and Evolution, 13, 1508-1527, 2022.
Kuo, S.: Phosphorus: Ascorbic acid method, in: Methods of Soil Analysis, Part 3. Chemical Methods, SSSA Book Series, SSSA, ASA, Madison, USA, 909, 1996.
Lal, R.: Soil health and carbon management, Food and Energy Security, 5, 212-222, https://doi.org/10.1002/fes3.96, 2016.
Le Bissonnais, Y.: Aggregate stability and assessment of soil crustability and erodibility .1. Theory and methodology, European Journal Of Soil Science, 47, 425-437, 1996.
Lloyd, S. P.: Least squares quantization in PCM, Bell Lab, 1957.
Lowder, S. K., Skoet, J., and Raney, T.: The number, size, and distribution of farms, smallholder farms, and family farms worldwide, World development, 87, 16-29, 2016.
MacQueen, J.: Some methods for classification and analysis of multivariate observations, Proceedings of the Fifth Berkeley Symposium on Mathematical Statistics and Probability,
Manić, M., Đorđević, M., Đokić, M., Dragović, R., Kićović, D., Đorđević, D., Jović, M., Smičiklas, I., and Dragović, S.: Remote Sensing and Nuclear Techniques for Soil Erosion Research in Forest Areas: Case Study of the Crveni Potok Catchment, Frontiers in Environmental Science, Volume 10 - 2022, 10.3389/fenvs.2022.897248, 2022.
Messinger, J. and Winterbottom, B.: African forest landscape restoration initiative (AFR100): restoring 100 million hectares of degraded and deforested land in Africa, 2016.
Moll, H. A. J.: Costs and benefits of livestock systems and the role of market and nonmarket relationships, Agricultural Economics, 32, 181–193, 2005.
Mullah, J. A., Ngonga, B. O., and Bii, W.: The impact of livestock grazing on forest structure, ground flora and regeneration of disturbed areas in Mau Forest, Kenya Forestry Research Institute Nairobi, Kenya2023.

Nzau, M., Mwangi, S. W., and Kinyenze, J. M.: Degradation of Grassland Ecosystems, Climate Change and Impacts on Pastoral Communities in Kenya, African Multidisciplinary Journal of Research, 3, 2018.
Olsen, S. R. and Sommers, L. E.: Phosphorus, in: Methods of Soil Analysis, 403-430, https://doi.org/10.2134/agronmonogr9.2.2ed.c24, 1982.
Owuor, S. O., Butterbach-Bahl, K., Guzha, A., Jacobs, S., Merbold, L., Rufino, M. C., Pelster, D. E., Díaz-Pinés, E., and Breuer, L.: Conversion of natural forest results in a significant degradation of soil hydraulic properties in the highlands of Kenya, Soil and tillage Research, 176, 36-44, 2018.
Pelster, D., Rufino, M., Rosenstock, T., Mango, J., Saiz, G., Diaz-Pines, E., Baldi, G., and Butterbach-Bahl, K.: Smallholder farms in eastern African tropical highlands have low soil greenhouse gas fluxes, Biogeosciences, 14, 187-202, 2017.
Quinton, J. N. and Fiener., P.: Soil erosion on arable land: An unresolved global environmental threat, Progress in Physical Geography: Earth and Environment, 48, 136-161, 2024.
R. Core Team: R: A Language and Environment for Statistical Computing, 2023.
Rufino, M. C., Atzberger, C., Baldi, G., Butterbach-Bahl, K., Rosenstock, T. S., and Stern, D.: Targeting landscapes to identify mitigation options in smallholder agriculture, Methods for Measuring Greenhouse Gas Balances and Evaluating Mitigation Options in Smallholder Agriculture, 15-36, 2016.
Rulinda, C. M., Dilo, A., Bijker, W., and Stein, A.: Characterising and quantifying vegetative drought in East Africa using fuzzy modelling and NDVI data, Journal of Arid Environments, 78, 169-178, 2012.
Scrucca, L., Fraley, C., Murphy, T. B., and Raftery, A. E.: Model-Based Clustering, Classification, and Density Estimation Using mclust in R, Chapman and Hall/CRC, 10.1201/9781003277965, 2023.
Steinley, D.: K-means clustering: A half-century synthesis, British Journal of Mathematical and Statistical Psychology, 59, 1-34, 10.1348/000711005X48266, 2006.
Sun, S. and Chen, S. S.: Extensive Decline of Soil Nitrogen and Its Drivers in the Lake Victoria Basin of Tropical Africa (1996–2015), Land Degradation & Development, 36, 5911-5926, https://doi.org/10.1002/ldr.70045, 2025.
Tagesson, T., Fensholt, R., Guiro, I., Rasmussen, M. O., Huber, S., Mbow, C., Garcia, M., Horion, S., Sandholt, I., Holm-Rasmussen, B., Göttsche, F. M., Ridler, M. E., Olén, N., Lundegard Olsen, J., Ehammer, A., Madsen, M., Olesen, F. S., and Ardö, J.: Ecosystem properties of semiarid savanna grassland in West Africa and its relationship with environmental variability, Global Change Biology, 21, 250-264, 2015.
Tate, K. R.: Microbial Biomass: A Paradigm Shift in Terrestrial Biogeochemistry, WORLD SCIENTIFIC (EUROPE), 348 pp., doi:10.1142/q0038, 2017.
Tibshirani, R., Walther, G., and Hastie, T.: Estimating the Number of Clusters in a Data Set Via the Gap Statistic, Journal of the Royal Statistical Society Series B: Statistical Methodology, 63, 411-423, 10.1111/1467-9868.00293, 2001.
Todd, S. W., Hoffer, R. M., and Milchunas, D. G.: Biomass estimation on grazed and ungrazed rangelands using spectral indices, International Journal of Remote Sensing, 19, 427-438, 1998.
Tully, K., Sullivan, C., Weil, R., and Sanchez, P.: The State of Soil Degradation in Sub-Saharan Africa: Baselines, Trajectories, and Solutions, Sustainability, 7, 6523-6552, 2015.
United Nations decade on ecosystem restoration 2021-2030: https://www.decadeonrestoration.org/, last access: 23/4/2025.

Vågen, T.-G., Winowiecki, L. A., Tondoh, J. E., Desta, L. T., and Gumbricht, T.: Mapping of soil properties and land degradation risk in Africa using MODIS reflectance, Geoderma, 263, 216-225, https://doi.org/10.1016/j.geoderma.2015.06.023, 2016.
van de Koppel, J., Rietkerk, M., and Weissing, F. J.: Catastrophic vegetation shifts and soil degradation in terrestrial grazing systems, Trends Ecol. Evol., 12, 352-356, 1997.
Vavrek, M. J.: fossil: palaeoecological and palaeogeographical analysis tools, Palaeontologia Electronica, 14, 2011.
Wang, R., Sun, Y., Zong, J., Wang, Y., Cao, X., Wang, Y., Cheng, X., and Zhang, W.: Remote Sensing Application in Ecological Restoration Monitoring: A Systematic Review, Remote Sensing, 16, 2204, 2024.
Wessels, K. J., Prince, S. D., Malherbe, J., Small, J., Frost, P. E., and VanZyl, D.: Can human-induced land degradation be distinguished from the effects of rainfall variability? A case study in South Africa, Journal of Arid Environments, 68, 271-297, https://doi.org/10.1016/j.jaridenv.2006.05.015, 2007.
Xiao, X., Hagen, S., Zhang, Q., Keller, M., and Moore, B.: Detecting leaf phenology of seasonally moist tropical forests in South America with multi-temporal MODIS images, Remote Sensing of Environment, 103, 465-473, 2006.
Yi, X., Li, G., and Yin, Y.: The impacts of grassland vegetation degradation on soil hydrological and ecological effects in the source region of the Yellow River--A case study in Junmuchang region of Maqin country, Procedia Environmental Sciences, 13, 967-981, 2012.
Yu, H., Xu, J., Okuto, E., and Luedeling, E.: Seasonal response of grasslands to climate change on the Tibetan Plateau, PLoS One, 7, e49230, 2012.
Zeng, C., Zhang, F., Wang, Q., Chen, Y., and Joswiak, D. R.: Impact of alpine meadow degradation on soil hydraulic properties over the Qinghai-Tibetan Plateau, Journal of Hydrology, 478, 148-156, https://doi.org/10.1016/j.jhydrol.2012.11.058, 2013.
Zhou, W., Yang, H., Huang, L., Chen, C., Lin, X., Hu, Z., and Li, J.: Grassland degradation remote sensing monitoring and driving factors quantitative assessment in China from 1982 to 2010, Ecological Indicators, 83, 303-313, 2017.

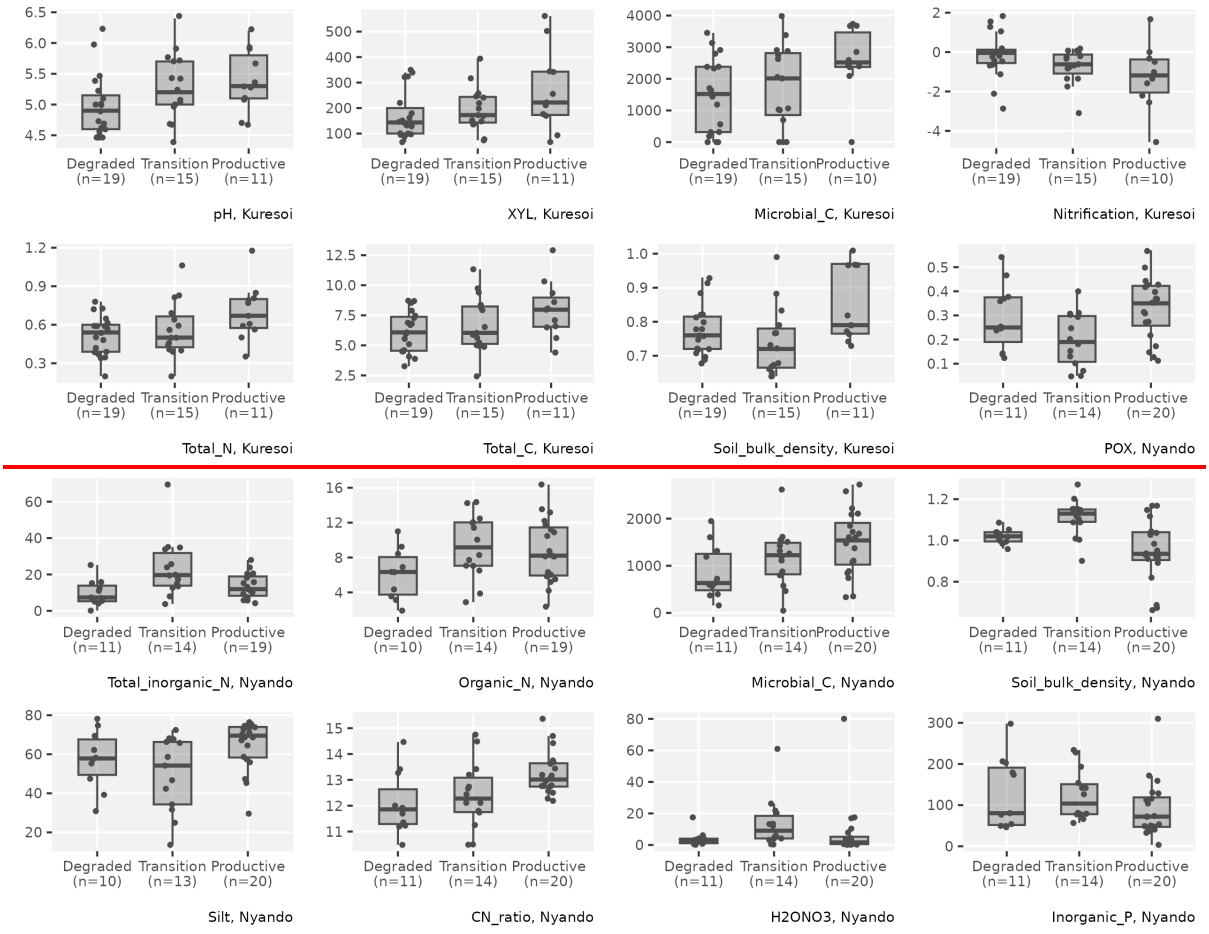

Figure 3: Boxplots of the soil variables with significant difference between degradation classes based on ANOVA or Kruskal-Wallis test from Kuresoi and Nyando respectively. The dark grey dots are the observations overlaid on top of the boxplots.

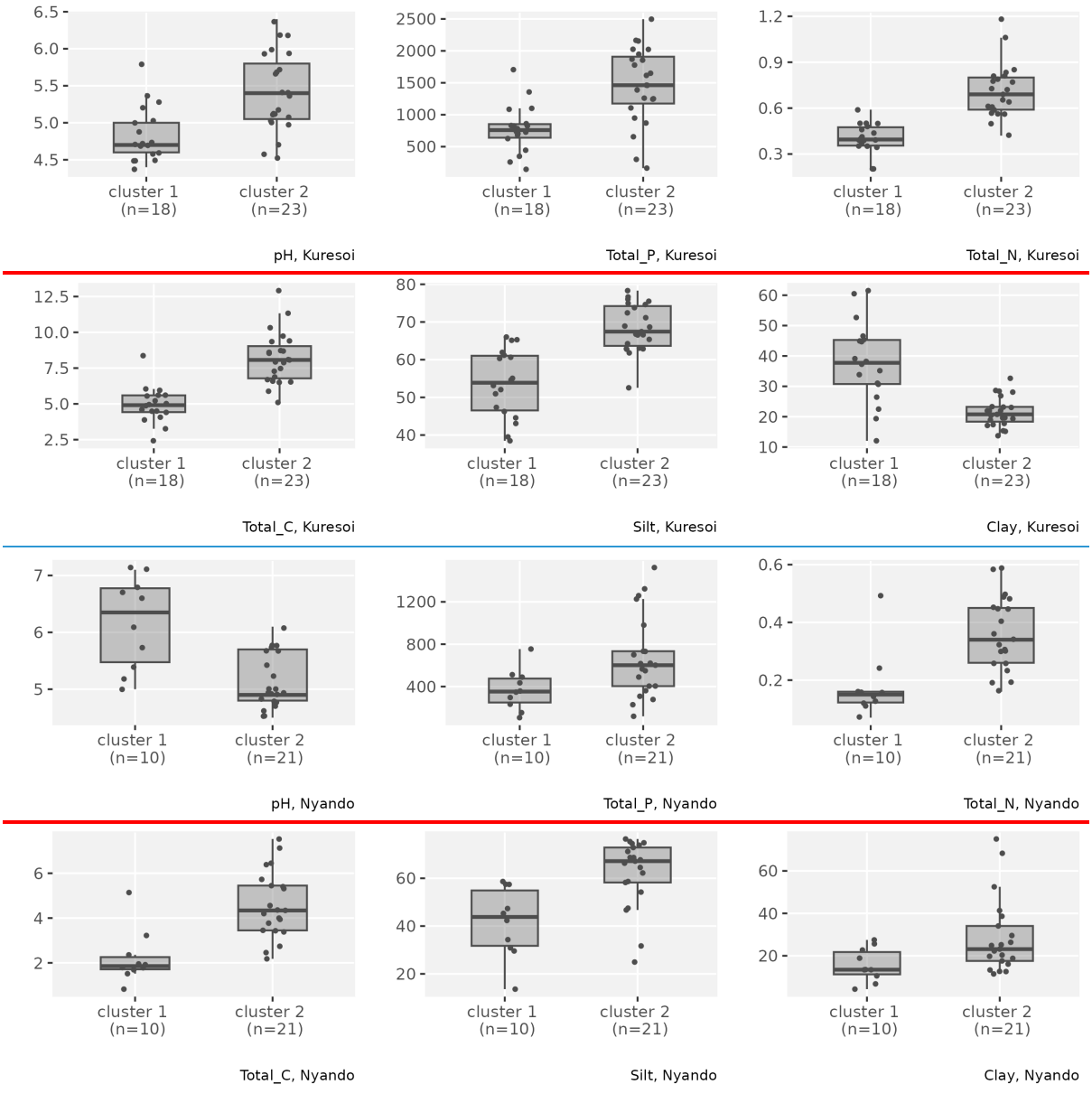

Figure S*: Box and whisker plots of selected stable variables that show a significant mean difference ($p<0.05$) between two clusters in both Kuresoi and Nyando, with observations (grey dots) overlaid on top.

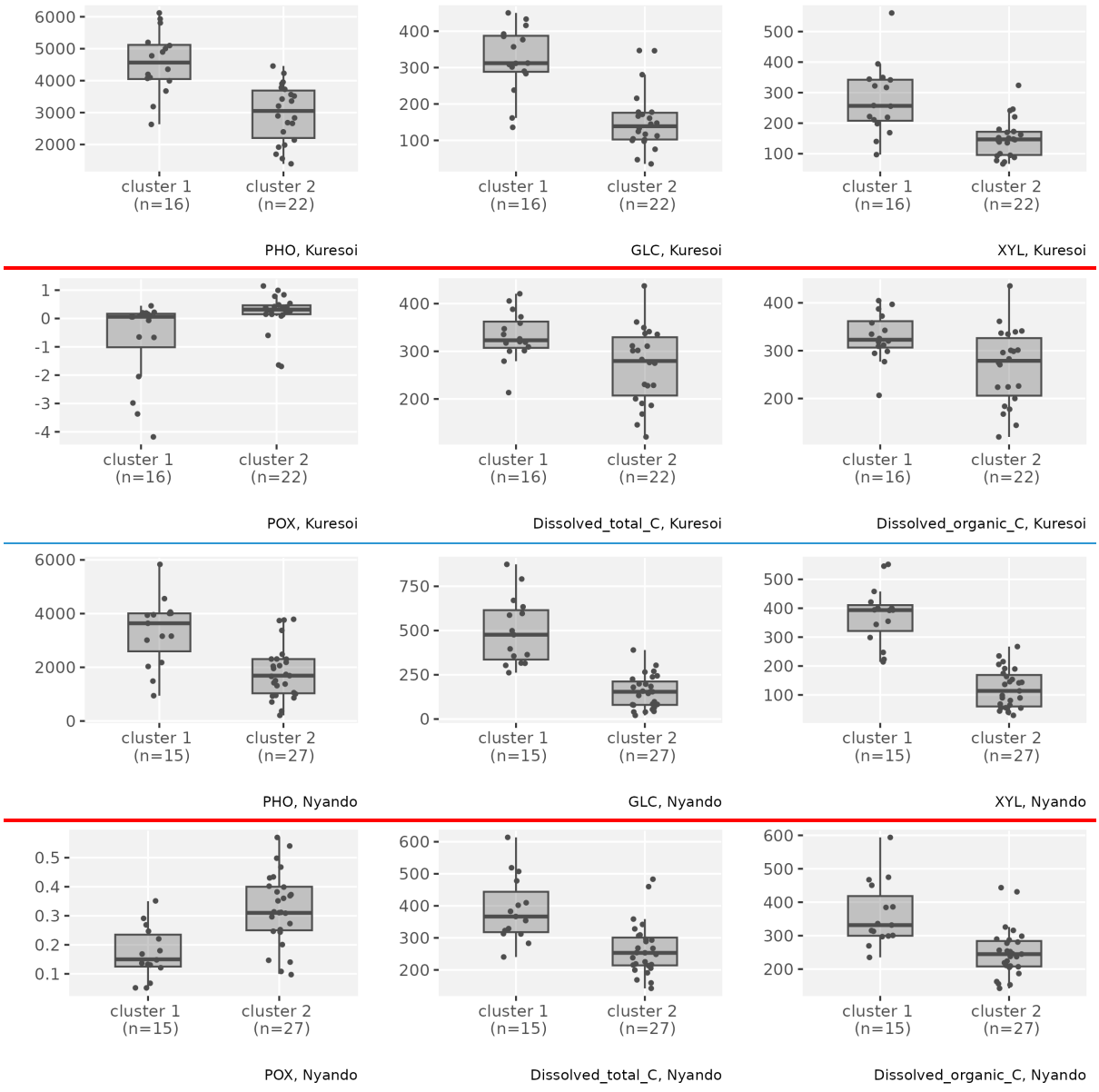

Figure S*: Box and whisker plots of selected transient variables that show a significant mean difference ($p<0.05$) between two clusters in both Kuresoi and Nyando, with observations (grey dots) overlaid on top.